Cooperative Relative Localization for UAV Swarm in GNSS-Denied Environment: A Coalition Formation Game Approach

Lang Ruan, Guangxia Li, Weiheng Dai, Shiwei Tian, Guangteng Fan, Jian Wang, *Member, IEEE*, and Xiaoqi Dai

***Abstract*—Unmanned aerial vehicle (UAV) swarms require accurate relative localization to safeguard flight missions in the global navigation satellite system-denied environment due to a lack of absolute position information. The existing work of relative localization faces challenges, such as the ranging information loss and the low localization frequency caused by long-distance ranging and large-scale characteristic of the UAV swarm. This article proposes a clustering-based cooperative relative localization scheme for UAV swarm, which contains a two-level framework: inter/intra-cluster localization. In order to investigate the tradeoff between intracluster cooperation and intercluster packet loss, the clustering-based problem is constructed as a coalition formation game (CFG) model. Given the designed coalition value, preference relation, and the coalition formation principles, it is proved that the proposed CFG model has a Nash stable partition. The designed coalition formation algorithm includes coalition heads and beacon drones selection mechanism. Simulation results show that the proposed CFG algorithms shorten the ranging time compared with global localization and achieve better localization performance (localization error and success rate) than contrast algorithms.**

***Index Terms*—Coalition formation games (CFGs), cooperative localization, global navigation satellite system (GNSS)-denied, unmanned aerial vehicle (UAV) relative localization.**

I. Introduction

POSITIONING, navigation, and timing (PNT) capabilities are essential to complement and support the global navigation satellite system (GNSS) system. In a GNSS-denied environment, signals can be obscured or jammed with for many reasons, including electromagnetic shielding, signal jamming, spoofing attacks, or other catastrophic GNSS failure events. For several years, civil/military groups have continued to call for various PNT methods, especially position acquisition, to achieve uninterrupted work in a GNSS-denied environment. Some promising solutions for localization have emerged.

Unmanned aerial vehicles (UAVs, also referenced as drones) have small sizes, strong mobility, and low cost. Owing to UAVs' wide range of military, public, and civil applications, UAV communication technology has also been rapidly developed [1]. Especially in a GNSS-denied environment, the rapidly changing scenario demands a high-speed and variable UAV swarm communication network to provide PNT capabilities. UAV swarms often need to obtain accurate location information while performing long-distance flight or launch formation to execute missions (e.g., monitoring, patrol, and rescue). Considerable research efforts have been devoted to UAV localization [2]–[6]. Mortier *et al.* [2] designed a navigation system based on time of arrival (TOA) and proposed a robust filtering method for ultrawideband (UWB) ranging. Minaeian *et al.* [3] utilized a UAV to execute a surveillance mission and proposed a comprehensive vision-based crowd detection and GIS localization algorithm for unmanned ground vehicles (UGVs). In [4], to accurately locate an interference source from a distance, Wu *et al.* proposed a multimodel Q-learning framework to realize UAV localization. Liu *et al.* [5] developed a distributed algorithm for a 3-D UAV relative localization network, which first obtains the local geometry through a weighted semidefinite programming (SDP) and then merges it into a global geometry based on statistical information. Arafat and Moh [6] proposed a swarm-intelligence-based localization (SIL) approach; they adopted clustering schemes for UAV networks in emergency communications, then convergence time and localization accuracy are improved with lower computational cost.

Nevertheless, there exist many challenges for UAV swarm localization and communication, such as mission requirements, complex and changeable electromagnetic environment, energy bottlenecks, the airborne devices constraint, etc. [7], [8]. On the one hand, control command dispatches for swarm occupy many communication resources, resulting in the contradiction between UAV swarm communication and localization. On the other hand, environmental factors, such as multipath, path fading, noise, and even substantial interference, severely restrict drones' absolute position acquisition and

Manuscript received May 22, 2021; revised October 31, 2021; accepted November 19, 2021. Date of publication November 23, 2021; date of current version June 23, 2022. This work was supported by the National Natural Science Foundation of China under Grant 61931011. *(Corresponding author: Shiwei Tian.)*

Lang Ruan, Guangxia Li, Weiheng Dai, and Xiaoqi Dai are with the College of Communications Engineering, Army Engineering University of PLA, Nanjing 210000, China (e-mail: ruanlangjyy@163.com; satlab13905177686@163.com; dwh_526@126.com; xiaoqi_dai@126.com).

Shiwei Tian is with the College of Communications Engineering, Army Engineering University of PLA, Nanjing 210000, China, and also with the National Innovation Institute of Defense Technology, Academy of Military Sciences, Beijing 100000, China (e-mail: wxzd2018@126.com).

Guangteng Fan and Jian Wang are with the National Innovation Institute of Defense Technology, Academy of Military Sciences, Beijing 100000, China (e-mail: fanguangteng@163.com; wangjian710108@126.com).

Digital Object Identifier 10.1109/JIOT.2021.3130000

ranging. Therefore, it is necessary to study reliable and practical solutions to achieve efficient relative localization of the UAV swarm.

Multiple dimensional scaling (MDS) [9] has proved promising for relative localization, which can get the relative position of the whole network without anchors. Above all, relative positions need to be transformed into positions in a known spatial coordinate system to facilitate subsequent processing. Much work so far focuses on collaborative network localization; they add nodes with known position information and mathematically map the relative positions of all nodes to the coordinate system they require [10]–[13]. Procrustes analysis [14]–[17] is one of the most widely used linear transformation methods in mapping positions. Mathematically speaking, it is the process to find the canonical shape and use the least-square (LS) method to find the affine change from each sample shape (relative position) to this standard shape (position in a required coordinate system).

We summarize that two characteristics of UAV swarm under mission requirements bring challenges for MDS: 1) *large-scale:* given the number of node n, the time complexity is $O(n^3)$. When n increases, the computational efficiency will decrease significantly and 2) *long-distance ranging:* MDS requires a complete ranging matrix, and long distances among drones will cause packet loss and make the ranging matrix incomplete. One improvement is to explore distance correction approaches among nodes in multihop networks, mainly including the weighting of the distance and the distance correction or replacement of the shortest path algorithm [10]–[12]. Even so, the above distance correction approaches in the irregular network topology will produce significant localization errors. MDS-MAP [9], [18] is an improved localization method based on MDS. It adopts clustering of transforming the global network into a regional subnetwork to reduce the algorithm's time complexity. Several works of MDS-MDP study UAV localization based on the existing ranging information [13], [19], [20]. The steps of MDS-MAP are normally as follows [9]: 1) set the range for local maps; 2) compute local maps for individual nodes; 3) merge local maps; and 4) transform the global map to an absolute map. Notably, MDS-MAP utilizes distance-based clustering to divide UAV global ranging into the local maps ranging (formed by close-range nodes), thereby effectively reducing the ranging packet loss caused by the long-distance ranging. For instance, Zhang *et al.* [20] presented a singular value decomposition (SVD)-MDS approach for EDM completion, which consists of the SVD-reconstruct algorithm. However, almost all work has preset the range for local maps formation, which cannot adapt to different scenarios. Meanwhile, in a GNSS-denied environment, the lack of anchors causes the global map to be unable to be transformed into an absolute map.

It should be noted that UAV swarm relative localization is a typical distributed multiagent control system, where players make decisions through interactive information, which is in line with the idea of game theory. The critical issue is how drones perform cooperative localization and how to correct ranging information through cooperation. Coalition formation games (CFGs) are typical cooperative games with solid potential in modeling problems in wireless communication networks [21], [22]. In CFGs, the network forms coalitions according to the players' preferences. For MDS-MAP, CFGs can constitute a practical analytical framework. The dynamic CFGs also contain many algorithms and concepts, which can be customized and adjusted for localization applications [23]. Therefore, clustering approaches in MDS-MAP can be described as a CFG, which serves as a theoretical guide for the UAV swarm cooperative localization scheme.

Under the condition of a GNSS-denied environment, this article aims to achieve accurate UAV swarm relative localization employing reasonable clustering and inter/intra-cluster localization based on the relative ranging information of the UAV swarm. To achieve this goal, we consider the performance of communication and ranging and propose a cooperative relative localization scheme for UAV swarm based on the CFG, and the work is described as follows.

1) We divide UAV swarm into different clusters by received signals among drones, then convert the localization problem into two-level localization: a) intercluster and b) intracluster relative localization. This clustering method lowers the complexity of the MDS algorithm since the dimensions of the ranging matrices reduce.
2) The proposed clustering problem is constructed as a CFG model. By setting a proper coalition value function, preference relations, and forming/breaking rules for coalitions, we prove the stable coalition structure of this model. In addition, the cluster-head selection method is designed considering communication utility.
3) After CFG-based clustering, a novel cooperative localization scheme is adopted, consisting of double-sided two-way ranging (DS-TWR) to shorten the ranging time and improve the localization frequency. A ground station (GS)-based local coordinate system is built to obtain the "absolute position" of beacon points. Finally, an MDS-MAP relative localization method based on matrix completion is designed to finish global network localization.

The main differences between this article and existing works are as follows: 1) unlike the traditional MDS-MAP with preset clustering, the proposed CFG scheme can adaptively form different clusters based on the received signal and has good robustness; 2) this article investigates the excessive packet loss caused by long-distance communication, mainly utilizing distance-related parameters to measure localization performance; and 3) this article studies the relative localization scheme based on any deployment location and topology of the UAV swarm, which could potentially be a fundamental guarantee for the research of mission-driven localization schemes.

In addition to Section I, the overview of this article is organized as follows: Section II gives the system scenario, the construction of clustering-based UAV swarm cooperative localization system model, and problem formulation. In Section III, basic notions of the coalitional game are first introduced, then the proposed clustering-based UAV swarm model is constructed as a CFG, and its stable state is analyzed based on given coalition order and preference relation. Based

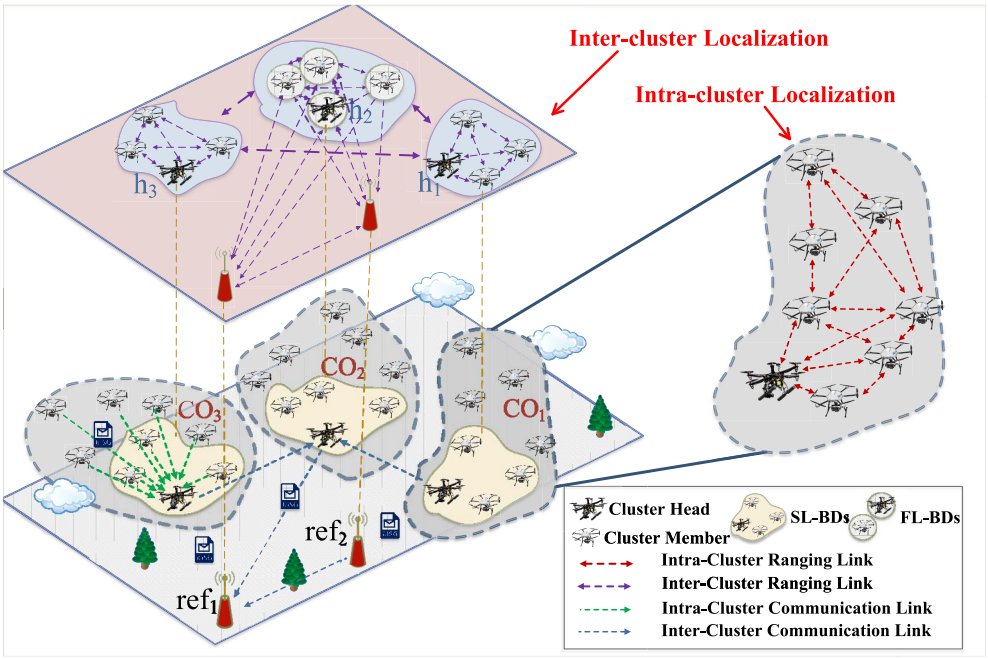

Fig. 1. Schematic of clustering-based UAV swarm cooperative localization in a mission area.

on CFG, Section IV designs a novel cooperative localization scheme, where different algorithms are designed to execute clustering and localization. Section V demonstrates the simulation results and gives analysis. Finally, the concluding remarks are given in Section VI.

II. System Model and Problem Formulation

Consider a GNSS-denied scenario where the UAV swarm performs cooperative localization to serve their mission requirements. With GNSS denied, drones cannot receive ranging information from satellites. Thus, mutual ranging information among UAV swarm is required to complete relative localization. Assume the set of UAV swarm in the whole network is defined as $\mathcal{N} = \{1, 2, \ldots, N\}$. Drones use sensor devices installed on their fuselage to perform ranging, positioning calculations, and data transmission.

Since the system carries out actual ranging processes in different periods, we evenly divide the mission duration of the UAV into T discrete time, which also reduces the decision-making space. The time set is defined as $\mathcal{T} = \{1, 2, \ldots, T\}$, of which the element is called a time slot $t \in \mathcal{T}$ (or a slot). Set the UAV n's 3-D position at the tth slot as $\mathbf{p}_{n,t} = [x_{n,t}, y_{n,t}, z_{n,t}], n \in \mathcal{N}, t \in \mathcal{T}$, where the elevation $z_{n,t}$ can be obtained from the barometer equipped on drones. The Euclidean geometric distance between UAV n and UAV $k \in \mathcal{K}$ is characterized as $d_{n,k} = \|\mathbf{p}_n - \mathbf{p}_k\|$, with $\|\cdot\|_2$ the L2-norm. In this article, symmetric DS-TWR is introduced. Two round-trip time measurements are used and combined together to obtain a time-of-flight (TOF) result to reduce error even for relatively long response delays. The measurement error dependent on the clock drift of ranging devices [24]. In that case, assume the measurement noise from UAV n to UAV k obey Gaussian distribution, that is, $u_{n,k} = N(0, \sigma_{n,k}^2)$, then the ranging measurement between two drones is given by

$$r_{n,k} = d_{n,k} + \mu_{n,k}. \tag{1}$$

Followed by (1), the relative observation Euclidean distance matrix (O-EDM) of the UAV swarm $\mathbf{D}_{\text{obs}} \in \mathbb{R}^{N\times N}$ is written as

$$\mathbf{D}_{\text{obs}} = \begin{bmatrix} 0 & r_{1,2} & \cdots & r_{1,N-1} & r_{1,N} \\ r_{2,1} & 0 & \cdots & r_{2,N-1} & r_{2,N} \\ \vdots & \vdots & \ddots & \vdots & \vdots \\ r_{N-1,1} & r_{N-1,2} & \cdots & 0 & r_{N-1,N} \\ r_{N,1} & r_{N,2} & \cdots & r_{N,N-1} & 0 \end{bmatrix}_{N\times N}. \tag{2}$$

The UAV swarm's large-scale nature causes them to take much time to measure and acquire EDM. Meanwhile, UAV swarm localization approaches require data transmission after completing ranging and relative localization. Due to the enormous energy consumption caused by long-distance transmission, specific drones can be assigned as relays to execute data forwarding [25]. In this way, the data collected by the UAV swarm will be forwarded to the control center for processing through the UAV communication link.

To address the above challenges, we adopt a clustering-based communication and localization approach, the specific implementation is described as follows: 1) select several drones as cluster heads (relays) for data forwarding and 2) employing intracluster and intercluster localization and alleviate the problem of ranging information packet loss caused by long distances. The proposed clustering-based approach can effectively reduce the acquisition time of the ranging message, thereby increasing the localization frequency throughout the network.

The schematic of the clustering-based localization process is shown in Fig. 1. In order to ensure an apparent display

effect, only part of the communication and ranging links are marked in this diagram. With the GNSS denied, there are no anchors with a known position, and traditional MDS cannot execute the coordinate mapping and output an intuitive coordinate map. In order to deal with the above problems, our proposed model constructs a space rectangular coordinate system based on the right-hand principle to achieve relative UAV swarm localization. The main elements of this diagram are as follows.

1) *Ground Stations:* Two GSs ref $= \{\text{ref}_1, \text{ref}_2\}$ are settled as beacons to determine the coordinate origin, x-axis, and y-axis. The drones' barometers obtain their altitudes to determine the z-axis. The detailed coordinate system construction process will be described in Section IV-C.
2) *Clusters:* All drones are divided into different clusters (i.e., formations), which are represented as $\mathcal{M} = \{1, 2, \ldots, M\}, 1 \leq M \leq N$. Denote $c_{n,t}$ as the cluster selected by UAV n, then for any cluster $m \in \mathcal{M}$, denote $\text{CO}_{m,t}$ as the UAV set belonging to this cluster, that is, $CO_{m,t} = \{n \in \mathcal{N} | c_{n,t} = m\}$. Each cluster m contains cluster beacon drones (BDs) and a cluster head drone $h_{m,t} \in CO_{m,t}$; the others are cluster member drones. Ranging information can be transmitted inside clusters (one-way arrow blue dotted line). Through cluster head drones, the ranging information and intracluster localization result transmission can be executed amongst clusters (one-way arrow green dotted line).
3) *Beacon Drones:* Inter/intra-cluster localizations require BDs. Suppose the BD set of cluster m at the tth time slot is $\{\text{ref}_{m,t}^{\text{inner}}\}_{m \in \mathcal{M}} \in CO_{m,t}$, the set of all BDs is $\text{ref}_t^{\text{inner}} = \sum_{m=1}^{M} \text{ref}_{m,t}^{\text{inner}}$. For BDs in all clusters (says CO_1, CO_2, and CO_3), they first execute intercluster localization (two-way arrow purple dotted line). These BDs serve as the relative anchors of their belonging cluster and execute intracluster localization (two-way arrow red dashed line). The detail of BDs will be described in Section II-B.

Unless otherwise specified, subsequent modeling and problem derivation are expressed at the tth time slot.

A. UAV Swarm Communication Modeling

Subject to UAV load restrictions, it is necessary to set up a control center to perform localization calculations and data backhaul. This control center can be a GS or a large drone. In this article, the GS is invoked as the control center. The UAV swarm transmits ranging information and communication data to the GS for processing through the inter/intra-clusters. It continues to execute data backhaul to realize global localization map upload. Data transmission performance among clusters mainly depends on the drones' parameters, communication distance, and channel conditions. The modeling process of the channel environment is given as follows.

UAV communicates through the air communication link, which makes the wireless channel open. This article adopts the block fading channel model based on the work in [26]. In this channel model, the characteristic parameters change over different slots. Since drones are relatively far from each other, the channel conforms to the characteristics of the small-scale fading model, which is configured on Rayleigh fading. Denote ε_t as the instantaneous fading coefficient, which obeys the exponential distribution of unit mean value. Assume the Euclidean geometric distance between UAV n and UAV k is denoted as $d_{n,k}(t)$, then the channel gain between UAV n and UAV k is given by

$$w_{n\to k}(t) = d_{n,k}^{\alpha}(t)\varepsilon_t \tag{3}$$

where α represents the fading path factor, due to the impact of small-scale fading, ε_t changes over time. Denote channel bandwidth and UAV n's transmit power as B and p_n, respectively, then by (3), for the signal received by UAV k from UAV n, the signal-to-noise ratio can be expressed as

$$\eta_{n\to k}\big(\mathbf{p}_{n,t}, \mathbf{p}_{k,t}, p_{n,t}\big) = \frac{p_{n,t} w_{n\to k}(t)}{N_0 B} \tag{4}$$

where N_0 represents the noise power per unit bandwidth. Then, maximum communication transmission rate (MCTR) UAV k's receiver received from UAV n's transmitter is then

$$R_{n\to k}\big(\mathbf{p}_{n,t}, \mathbf{p}_{k,t}, p_n\big) = B\log\big(1 + \eta_{n\to k}\big(\mathbf{p}_{n,t}, \mathbf{p}_{k,t}, p_n\big)\big). \tag{5}$$

Since DS-TWR and data backhaul links are both double-way, the communication rate between UAV n and UAV k can be given by the average value of the maximum communication rate of the signal received by these two drones from each other

$$\begin{aligned} R_{n,k}^{\text{double}}\left(\mathbf{p}_{n,t}, \mathbf{p}_{k,t}, p_n, p_k\right) = {} & \frac{1}{2} R_{n\to k}\big(\mathbf{p}_{n,t}, \mathbf{p}_{k,t}, p_n\big) \\ & + \frac{1}{2} R_{k\to n}\big(\mathbf{p}_{k,t}, \mathbf{p}_{n,t}, p_k\big). \end{aligned} \tag{6}$$

Let ref_1 denote No.1 GS, i.e., the command center. Thus, the maximum communication rate of the whole UAV network is then

$$\begin{aligned} & R_t^{\text{Com}}\big(\{\mathbf{p}_{n,t}\}_{n\in\mathcal{N}}, \{c_n\}_{n\in\mathcal{N}}, \{h_m\}_{m\in\mathcal{M}}\big) \\ & \quad = \sum_{m\in\mathcal{M}} \left(R_{h_m,\text{ref}_1}^{\text{double}}(\cdot) + \sum_{n\in CO_m\setminus\{h_m\}} R_{n,h_m}^{\text{double}}(\cdot) \right). \end{aligned} \tag{7}$$

There are two items in (7): the first item represents the MCTR from the cluster head drones to the GS and the second item represents the MCTR from cluster head drones to the other drones within the same clusters. The above equation shows that the maximum communication rate of the UAV network is determined by the current deployment position of drones and their cluster selection at the different time slots. It is worth noting that $R_t^{\text{Com}}(\cdot)$ characterizes the communication capability of the whole UAV network and plays a vital role in guaranteeing information in the mission-driven scenario.

B. UAV Swarm Inter/Intra-Cluster Relative Localization Modeling

After finishing clustering, the inter/intra-cluster relative localization model is constructed in this section (see from Fig. 1), and the performance is analyzed. It is known that given sufficient anchor nodes ($m+1$ or more for m-D networks), the positions of the anchors in the relative map can be mapped to their absolute positions through a linear transformation [9]. It

is generally accepted that GSs are always far away from the drones in flight missions, leading to incomplete O-EDM acquisition and thus restricting clustering. In 3-D UAV networks, the inter/intra-relative localization method is proposed to cope with this problem.

Intercluster Localization: For all cluster BDs, four BDs, which can be connected with the GSs for communication and ranging, are selected as the ground–air beacons. These BDs are called first-level BDs (FL-BDs). FL-BDs first obtain the position based on ranging information from the GSs, then complete relative localization with other BDs called the second-level BDs (SL-BDs).

Intracluster Localization: After completing relative localization among BDs, each cluster maps the absolute position of BDs to the other cluster member drones and finally completes global relative localization through data transmission.[1]

The inter/intra-cluster localization algorithm is introduced in Section IV-A, and suppose FL-BDs are located in cluster $m^* \in \mathcal{M}$. Intuitively, the amount of clusters and cluster members is the optimization variable of the proposed clustering problem, which affects the cluster localization performance through the following factors: 1) ranging packet loss; 2) cluster localization accumulative error; and 3) localization frequency. The problem is outlined as follows.

1) Ranging Packet Loss: Ranging packet loss leads to incomplete O-EDMs. First, to characterize the ranging packet loss among drones, denote the ranging signal-to-noise ratio of from UAV n to UAV k as follows:

$$\eta^{\text{loc}}_{n\to k}\left(\mathbf{p}_{n,t}, \mathbf{p}_{k,t}, p_n\right) = \begin{cases} \eta_{n\to k}\left(\mathbf{p}_{n,t}, \mathbf{p}_{k,t}, p_n\right), & \eta_{n\to k}\left(\mathbf{p}_{n,t}, \mathbf{p}_{k,t}, p_n\right) \geq \eta_0 \\ 0, & \eta_{n\to k}\left(\mathbf{p}_{n,t}, \mathbf{p}_{k,t}, p_n\right) < \eta_0 \end{cases} \tag{8}$$

where η_0 is the demodulation threshold of the ranging signal. Since two-way ranging requires both links to be able to demodulate the ranging signal and read the time stamp in it, so the ranging signal-to-noise ratio of UAV n and UAV k is represented as $\eta^{\text{loc}}_{n,k}(\mathbf{p}_{n,t}, \mathbf{p}_{k,t}, p_n) = \min(\eta^{\text{loc}}_{n\to k}(\cdot), \eta^{\text{loc}}_{n\to k}(\cdot))$, abbreviated as $\eta^{\text{loc}}_{n,k}(t)$. Obviously, $\eta^{\text{loc}}_{n,k}(t) = \eta^{\text{loc}}_{k,n}(t)$. In that case, the ranging packet loss among all drones in cluster m is characterized as $f_t(m) = \sum_{n,k\in CO_m} f(\eta^{\text{loc}}_{n,k}(t))$, where $f(\eta^{\text{loc}}_{n,k}(t))$ is the indicator function

$$f\left(\eta^{\text{loc}}_{n,k}(t)\right) = \begin{cases} 0, & \eta^{\text{loc}}_{n,k}\left(\mathbf{p}_{n,t}, \mathbf{p}_{k,t}, p_n\right) \geq \eta_0 \\ 1, & \eta^{\text{loc}}_{n,k}\left(\mathbf{p}_{n,t}, \mathbf{p}_{k,t}, p_n\right) < \eta_0. \end{cases} \tag{9}$$

According to (9), $f_t(m)$ represents the number of lost ranging packets among drones in cluster m.

2) Cluster Localization Accumulative Error: The results of intracluster (intercluster) localization are calculated based on the ground-to-air (intracluster) localization results. Therefore, localization errors will be accumulated in the next level of localization.[2] According to (8), the ranging rate of UAV n and UAV k is

$$R^{\text{loc}}_{n,k}\left(\mathbf{p}_{n,t}, \mathbf{p}_{k,t}, p_n\right) = B\log\left(1 + \eta^{\text{loc}}_{n,k}\left(\mathbf{p}_{n,t}, \mathbf{p}_{k,t}, p_n\right)\right). \tag{10}$$

It can be seen that ranging communication rate has a negative correlation with the ranging packet loss. Hence, $R^{\text{loc}}_{n,k}$ can be utilized to characterize localization accumulative error. Change drones to the GSs, (10) also holds, the corresponding derivation is the same as above. Therefore, define the set of FL-BDs as $\text{ref}^{\text{inner}}_{m^*,t}$, then the ranging utility between the FL-BD $j \in \text{ref}^{\text{inner}}_{m^*,t}$ and the GSs *ref* is expressed as

$$U^{\text{LocOuter}}_j\left(\mathbf{p}_{j,t}, p_j\right) = \frac{\sum_{\xi\in\text{ref}} R^{\text{loc}}_{\xi,j}}{\sum_{j\in\text{ref}^{\text{inner}}_{m^*,t}} f\left(\eta^{\text{loc}}_{j,\text{ref}}(t)\right)}. \tag{11}$$

When other parameters remain unchanged, the larger the ranging utility value, the larger the ranging rate value among drones, and the less the ranging packet loss. It can also be seen from (3) and (4) that the Euclidean distance value among drones is also shorter. The shorter the Euclidean distance, the shorter the ranging response time between nodes, effectively reducing the localization error for some ranging schemes (e.g., single-sided two-way ranging, SS-TWR). It can be concluded from (10) that the utility of ranging information among all BDs (excluding beacon members of the same cluster) is expressed as

$$\begin{aligned} &U^{\text{LocInter}}\left(\left\{\mathbf{p}_{n,t}\right\}_{n\in\mathcal{N}}, \left\{c_{n,t}\right\}_{n\in\mathcal{N}}\right) \\ &= \sum_{i\in\text{ref}^{\text{inner}}_t} U^{\text{LocInter}}_i(\cdot) \\ &= \frac{\sum_{i\in\text{ref}^{\text{inner}}_t}\sum_{j\in\text{ref}^{\text{inner}}_t\setminus\left\{\text{ref}^{\text{inner}}_{c_i,t}\right\}} R^{\text{loc}}_{j,i}(\cdot)}{\sum_{n,k\in\text{ref}^{\text{inner}}_t} f\left(\eta^{\text{loc}}_{n,k}(t)\right)}. \end{aligned} \tag{12}$$

Similarly, for all the drones in cluster m, the sum of ranging utility among them is then

$$U^{\text{LocIntra}}_m\left(\left\{\mathbf{p}_{n,t}\right\}_{n\in\mathcal{N}}, \left\{c_{n,t}\right\}_{n\in\mathcal{N}}\right) = \frac{\sum_{n\in CO_m}\sum_{k\in CO_m\setminus n} R^{loc}_{k,n}(.)}{2\cdot f_t(m)}. \tag{13}$$

Therefore, in combination with (11)–(13), the total ranging utility of the UAV network is

$$\begin{aligned} &U^{\text{Loc}}_t\left(\{p_n\}_{n\in\mathcal{N}}, \left\{c_{n,t}\right\}_{n\in\mathcal{N}}, \left\{h_{m,t}\right\}_{m\in\mathcal{M}}, \left\{\text{ref}^{\text{inner}}_{m,t}\right\}_{m\in\mathcal{M}}, m^*\right) \\ &= \sum_{j\in\text{ref}^{\text{inner}}_{m^*,t}} U^{\text{LocOuter}}_{j,\text{ref}}(\cdot) + U^{\text{LocInter}}(\cdot) + \sum_{m\in\mathcal{M}} U^{\text{LocIntra}}_m(\cdot). \end{aligned} \tag{14}$$

3) Localization Frequency: The DS-TWR scheme is introduced in this article to implement two-way ranging between two nodes (drones/GSs). Compared with the SS-TWR scheme, the DS-TWR scheme does not need to keep the response time unchanged, which gives excellent flexibility in the design of application scenarios. The error in the calculated TOF is also minimized. Compared with the SDS-TWR scheme, the DS-TWR scheme can significantly save information traffic, saving battery power and talk time. The drawbacks of

[1]To avoid confusion, when the absolute position (using quotation marks to indicate particularity) is mentioned, it refers to the relative position of the local coordinate system constructed based on GSs.

[2]On the premise that can be obtained from sensors onboard, parameters related to distance can also be used for measuring performance (e.g., signal energy and time difference of arrival).

the DS-TWR scheme are that it requires multiplication and division operations.

In the case of a point-to-point UAV localization network composed of N mobile nodes, each node hopes to obtain the distance from other nodes. Then, there are a total of $N(N-1)/2$ ranging measurements, described as $g(N)$. For example, for a 5-node network, there need ten ranging measurements. Suppose the cluster set of drones at the tth time slot is $\mathcal{M}_t \in \mathcal{M}$, then the location frequency of completing a global localization in the DS-TWR scheme can be described as $\text{fre}(\mathcal{M}_t)$. The value of $\text{fre}(\mathcal{M}_t)$ depends on the number of clusters and the number of cluster members because these factors directly affect the acquisition of ranging messages. Section IV-B shows a specific slot structure design and description.

In the whole ranging process, the ranging from ground-to-air, intercluster, and intracluster is serial, while the ranging within each intracluster is parallel. The amount of ranging messages required by the whole UAV network to complete a global localization mission is expressed as follows:

$$h(\mathcal{M}_t) = g(6) + g(4 \cdot \text{card}(\mathcal{M}_t)) + g\big(\max\big(\text{card}_{m\in\mathcal{M}_t}(CO_m)\big)\big). \tag{15}$$

In the above equation, the first item represents the ranging messages required between two GSs and four FL-BDs; the second item represents the ranging messages required to complete intercoalition localization; and the third item represents the maximum ranging messages required by the drones to complete intracoalition localization. The localization frequency $\text{fre}(\mathcal{M}_t)$ and $h(\mathcal{M}_t)$ is in anti-correlation.

4) Problem Objective: In the proposed model, the position and the transmit power of the UAV swarm $\{\mathbf{p}_{n,t}\}_{n\in\mathcal{N}}$ and $\{p_n\}_{n\in\mathcal{N}}$ are fixed at the tth time slot. Then, it can be concluded from (14) and $\text{fre}(\mathcal{M}_t)$ that the whole network's objective is to optimize drones' selections of clusters, cluster heads, FL-BDs, and SL-BDs to maximize the total ranging utility

$$\mathcal{P}_1 : \left[\{c_n\}_{n\in\mathcal{N}}, \{h_m\}_{m\in\mathcal{M}}, \left\{\text{ref}_m^{\text{inner}}\right\}_{m\in\mathcal{M}}, m^*\right] = \arg\max U_t^{Loc} \tag{16}$$

$$\text{subject to: } \text{CO}_m = \{n \in \mathcal{N} | c_n = m\} \tag{17a}$$

$$h_m \in CO_m \tag{17b}$$

$$\text{ref}_m^{\text{inner}} \in CO_m \tag{17c}$$

$$R_t^{Com}(\cdot) \geq R_{th1} \tag{17d}$$

$$fre(\mathcal{M}_t) \geq \text{fre}_{th}. \tag{17e}$$

Equations (17d) and (17e) represent that UAV swarm must meet the requirement of the whole network communication transmission rate and localization frequency, respectively.

The proposed UAV swarm clustering problem is a multiuser decision-making problem. In order to achieve $\mathcal{P}_1$, several points should be concerned.

1) The proposed model utilizes clustering to compress the acquisition amount of O-EDMs which can be able to complete localization, to alleviate the problem of ranging packet loss caused by large-scale UAV swarm localization.
2) Selections of FL-BDs and SL-BDs need to ensure successful communication and ranging to the greatest extent possible.
3) The number of clusters and cluster members affect the localization frequency and determine the amount of ranging information that can be obtained. Those two mutually restrict the localization error.

Based on the above description, CFGs are introduced to characterize and analyze the proposed problem. The following section designs a CFG approach for UAV swarm cooperative localization.

III. Coalition Formation Game Approach for Clustering-Based UAV Swarm Cooperative Localization

The proposed clustering-based UAV swarm localization model is a typical distributed multiagent control system, where players make decisions through interactive information and value their actions based on payoffs, which are in line with the idea of the game. Drones in cooperative localization are called players of the game. In the proposed model, players perform different cooperative localization missions with different players, making this model a cooperative game. The critical issue of cooperative games is how players cooperate and how to distribute the benefits after cooperation. Therefore, the proposed clustering-based UAV swarm cooperative localization model is constructed as a CFG in this section. First, several game concepts are given as follows.

A. Basic Notions of Coalitional Game

A coalitional game is denoted by the pair $(\mathcal{N}, V)$, where $\mathcal{N}$ is the player set, V is a mapping function, indicating the value of coalitions. The most common form of a coalitional game is the characteristic form [27]. Coalitional games with transferable utility (TU) or nontransferable utility (NTU) [28] constitute one of the most important and common types of cooperative games. In contrast, in NTU games, the payoff of each player in coalition CO depends on the joint actions taken by the players of coalition CO, i.e., the coalition value V cannot be assigned a single actual number, or the distribution of the payoff is under rigid restrictions.

Coalitional games in characteristic form focus on the stability of players in the grand coalition [29], [30]. Recently, coalitional games in partition form draw much attention to cooperative game theory and provide theoretical support for cooperation ways and payoff distribution of players.

Definition 1 (Coalition Partition [31], [32]): A *coalition partition* or a *coalition structure* is a set $\Pi = \{CO_m\}_{m=1}^{M}$ which partitions $\mathcal{N}$. Coalition $\text{CO}_m \in \mathcal{N}$ are disjoint and $\cup_{m=1}^{M} CO_m = \mathcal{N}$. Specifically, Π is called the *grand coalition* when $M = 1$. Given a coalition partition Π and a player $n \in \mathcal{N}$, let $\text{CO}_\Pi(n)$ denote all players of the coalition where n belongs, which is $\text{CO}_\Pi(n) = \text{CO}_{c_n}$.

Definition 2 (Coalitional Game in Partition Form [33]): A coalitional game $(\mathcal{N}, V)$ is said to be in *partition form* if V is denoted by $V(\text{CO}, \Pi) \in \mathbb{R}^{|\text{CO}|}$. That is, for $\Pi \in \Psi$ (Ψ is the set of all possible partitions) and coalition $\text{CO} \in \mathcal{N}$,

$V(\mathrm{CO}, \Pi)$ represents the payoff vector that can be achieved by not only the strategies of players in coalition CO but also the strategies of players in other coalition $\Pi \backslash \mathrm{CO}$.

For a coalitional game in partition form, its payoff depends on how the network is divided, i.e., network structure and cost for cooperation play a significant role. In this regard, coalitional games in partition form are often classified as CFGs [23].

Definition 3 (Coalition Formation Game [31]): A (hedonic) *CFG* is given by a pair $(\mathcal{N}, (\succeq_n)_{n\in\mathcal{N}})$, where $\succeq_n$ is a reflexive, complete, and transitive binary relation, denoting player n's *preference relation* or *order*. We let $\succ_n$ denote the associated asymmetric binary relation.

For arbitrary player $n \in \mathcal{N}$, given two coalitions CO_1 and CO_2 and their respective partitions Π and Π' $(\Pi, \Pi' \in \Psi)$. While other players $\mathcal{N}\backslash n$ stay the same coalition selections, $\mathrm{CO}_1 \succ_n \mathrm{CO}_2$ indicates that player n prefers to be part of coalition CO_1 when Π is in place, over being part of coalition CO_2 when Π' is in place.

B. Clustering-Based UAV Swarm Localization Model Constructed as Coalition Formation Game

First, the proposed model is characterized as a coalitional game $\mathcal{G}$, which is

$$\mathcal{G} = \left(\mathcal{N}, \{s_n\}_{n\in\mathcal{N}}, V\right). \tag{18}$$

1) $\mathcal{N} = \{1, 2, \ldots, N\}$ represents the players (drones) set.
2) $s_n = c_n \otimes al_n \otimes a2_n \otimes a3_n$ ($\otimes$ is the Cartesian product) is the set of all available strategies of UAV n, including available coalition $c_n \in C_n, C_n \subseteq \mathcal{M}$. $a1_n, a2_n$, and $a3_n$ are the indicator strategies. $a1_n = 1$ indicates that UAV n is the coalition head, $a1_n = 0$ indicates that the UAV is not the coalition head; similarly, $a2_n$ and $a3_n$ indicate whether UAV n is SL-BD and FL-BD or not, respectively. Define $s_{-n} \in s_1 \otimes s_2 \otimes \cdots \otimes s_{n-1} \otimes s_{n+1} \otimes \cdots \otimes s_N$ as collections of strategies for all drones except UAV n, so are c_{-n}, $a1_{-n}$, $a2_{-n}$, and $a3_{-n}$.
3) $V(\mathrm{CO}, \Pi)$ is the utility function, indicating the total payoff generated by any coalition CO and is characterized as

$$V(CO, \Pi) = \left\{ u(CO, \Pi) \in \mathbb{R}^{|S|} | u(\cdot) = \sum_{n\in CO} u_n(s_n, s_{-n}) \right\}. \tag{19}$$

Equation (19) represents that for a coalition partition Π, when acting in coalition CO, V is a real number describing the utility that coalition CO receives and is numerically the same as the sum of utility of the players in coalition CO, which means V is determined by the joint action $\{s_n\}_{n\in\mathrm{CO}}$ of players in coalition CO. What is more, V cannot be distributed in any arbitrary manner among the members of CO, then the proposed game $\mathcal{G}$ has NTU. Given $\{\mathbf{p}_n\}_{n\in\mathrm{CO}}$, the whole ranging utility is expressed as (20), shown at the bottom of this page, which represents that if UAV n's coalition is the one contains FL-BDs ($c_n = m^*$), the whole ranging utility is the sum of SL-BDs and c_n's intracoalition ranging utility. Otherwise, the whole ranging utility is the sum of GS-to-FL-BDs, SL-BDs, and c_n's intracoalition ranging utility.

Thus, the payoff of every player $n \in \mathcal{N}$ in the coalition depends on the partition Π, from Definition 2, we have the following.

Due to the improvement of ranging utility brought by players' cooperation, i.e., GSs and FL-BDs ranging, intercoalition ranging, and intracoalition ranging, the completeness of O-EDMs is ensured, thus improving the localization performance. In the meantime, the grand coalition seldom benefits from packet loss (reflected as a decrease in ranging utility) caused by long-distance ranging, and their formation is limited.

Remark 1: For the proposed coalitional game in partition form $\mathcal{G}$, its dependence on externalities and the benefit–cost tradeoff of cooperation is reflected in (11)–(14), and any coalition structure may be formed in the network. Therefore, the proposed clustering-based UAV swarm cooperative localization game model is classified as a CFG.[3]

CFGs are inherently complex to solve. In order to explore a benefit–cost tradeoff cooperation, i.e., the optimal coalition structure, centralized approaches can be used, which is usually NP-complete. To find the optimal coalition structure, all partitions of player $\mathcal{N}$ need to be iterated, which makes the iteration times increase exponentially. Therefore, finding the optimal coalition structure using a centralized method is often computationally complex and impractical. Inspired by the work of [23] and [30], we follow the general principles of the coalition formation algorithm they provided in this article. By exploring the characteristics of CFGs, especially the coalition value V, the coalition formation process takes place in a distributed manner. Players can independently decide whether to join the coalition to reduce the centralized complexity. Significantly, three elements need to be taken concern while designing the dynamic coalition formation algorithm: 1) restrict preference orders over the coalitions; 2) rules for forming/breaking coalition; and 3) assess the stability of partitions.

C. Preference Orders

From Definition 3, we know that each player has preferences over possible coalition partitions, which are entirely determined by the coalition selections of all the players. Thus, preference in CFG is an essential basis to determine the coalition structure. Utilitarian order [34] and Pareto order [30] are

[3]In order to unify the expression, we will use "coalition" to replace "cluster" in the following. For instance, inter/intra-coalition refer to inter/intra-cluster.

$$\sum_{n\in\mathrm{CO}} u_n(s_n, s_{-n}) = \begin{cases} \frac{1}{2} U^{\mathrm{LocInter}}(\cdot) + U_{c_n}^{\mathrm{LocIntra}}(\cdot), & c_n \neq m^* \\ \sum_{j\in \mathrm{ref}_{m^*,t}^{\mathrm{inner}}} U_{j,\mathrm{ref}}^{\mathrm{LocOuter}}(\cdot) + \frac{1}{2} \cdot U^{\mathrm{LocInter}}(\cdot) + U_{c_n}^{\mathrm{LocIntra}}(\cdot), & c_n = m^* \end{cases} \tag{20}$$

the most common preference orders for comparing collections of the coalition. However, utilitarian order cannot apply to NTU games. With Pareto order, UAV n complete the coalition selection, while neither the payoff of the drones in its original coalition CO nor that in its new coalition $CO_{\prime}$ will be damaged, $CO, CO' \in \Pi$. This characteristic ensures that the overall payoff of the coalition structure Π will never fall, which provides ample theoretical support for the proof of the stable partition. The Pareto order is available for both TU and NTU games [23]. Regrettably, Pareto order cannot guarantee the optimal solution to the problem. In order to solve the optimal coalition structure of the proposed NTU game, motivated by the work in [35], a new preference order is introduced as follows.

Definition 4 (Coalition Order): The preference relation of a CFG satisfies coalition order if, for arbitrary player $n \in \mathcal{N}$ and its two coalition selection c_n and c'_n, the group of players $\mathcal{N}$ prefers to organize themselves into a collection $\Pi = \{CO_1, \ldots, CO_{c_n} \cup n \ldots, CO_{c'_n} \ldots, CO_M\}$ instead of $\Pi^* = \{CO_1, \ldots, CO_{c_n} \ldots, CO_{c'_n} \cup n \ldots, CO_M\}$, i.e.,

$$\begin{aligned} \mathrm{CO}_{c_n} &\succ_n \mathrm{CO}_{c'_n} \\ &\Longrightarrow V\big(CO_{c_n} \cup \{n\}, \Pi\big) + V\big(CO_{c'_n}, \Pi\big) \\ &> V\big(\mathrm{CO}_{c_n}, \Pi^*\big) + V\big(CO_{c'_n} \cup \{n\}, \Pi^*\big). \end{aligned} \tag{21}$$

Thus, we characterize the utility function as $U(s_n, s_{-n}) = V(\mathrm{CO}_{c_n}, \Pi) + V(\mathrm{CO}_{c'_n}, \Pi)$ by coalition order, where c'_n represents the expect action.

Remark 2: Given coalition order and designed utility function $U(s_n, s_{-n})$, the proposed CFG $\mathcal{G}$ satisfies the characteristics of additive separable and symmetry.

Meanwhile, the properties of the coalition order can well prove the existence of the optimal coalition partition by mapping the system model's global utility to the UAV network's local utility. The specific proof process is characterized in Section III-E.

D. Rules for Forming/Breaking Coalitions

Apt and Witzel [34] introduced merge and split rules on forming coalition structure, as shown in Fig. 2. Based on these rules, drones in the same coalition will execute batch strategy changes. They may fall into a fixed combination with other drones once the initial coalition formation conditions are not good. In addition, in the later stages of the formation, the corresponding rules have very little impact on the coalition structure, which rides the implementation of the rules very difficult and leads to invalid calculations. In order to avoid these problems (partial traps, invalid calculations, etc.) caused by traditional rules, this section introduces the following rules for coalition selection.

Definition 5 (Coalition Selection Rule [36]): Given two coalition CO_m and $\mathrm{CO}_{m'}$, $m \neq m'$, for arbitrary player $n \in \mathcal{N}$, it prefers to choose to join the coalition CO_m if n prefers to be the part of CO_m over being $\mathrm{CO}_{m'}$ based on the given preference order, i.e.,

$$n \to \mathrm{CO}_m \Leftrightarrow \mathrm{CO}_m \succ_n \mathrm{CO}_{m'} \quad \forall \mathrm{CO}_m, CO_{m'} \in \Pi. \tag{22}$$

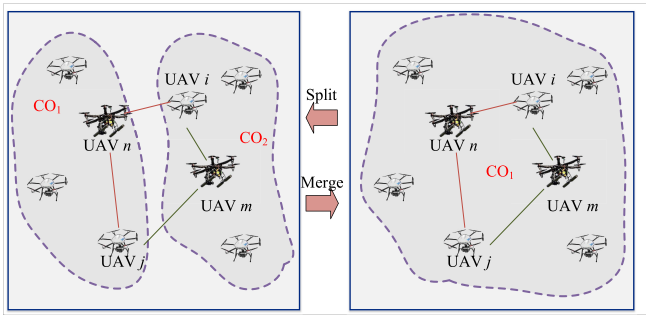

Fig. 2. Merge/split rule schematic.

Definition 6 (Switch Rule): Given two coalition CO_m and $\mathrm{CO}_{m'}$, $m \neq m'$, for arbitrary two players $n, k \in \mathcal{N}$, they prefer to choose to join the coalition CO_m and $\mathrm{CO}_{m'}$, respectively, if $n(k)$ prefers to be the part of $\mathrm{CO}_{c_k}(\mathrm{CO}_{c_n})$ over being $\mathrm{CO}_{c_n}(\mathrm{CO}_{c_k})$ based on the given preference order, i.e.,

$$\begin{aligned} n \to CO_{c_k}, k \to CO_{c_n} &\Leftrightarrow \mathrm{CO}_{c_k} \succ_n \mathrm{CO}_{c_n} \\ \mathrm{CO}_{c_n} \succ_k \mathrm{CO}_{c_k} \quad &\forall CO_{c_k}, CO_{c_n} \in \Pi. \end{aligned} \tag{23}$$

Remark 3: Given two coalitions CO_1 and CO_2, merge and split can be achieved by a certain number of coalition selection rules or switch rules.

Under those orders, the coalition selection mechanism can realize the functions of the two orders simultaneously while avoiding the batch strategy selection of UAVs. Therefore, even if the UAV's strategic choices have stalled, it may still be on track soon.

E. Analysis of the Stable Coalition Partition

The individual stability definitions are adapted from Dreze and Greenberg [37].

Lemma 1: If players' preferences are additively separable and symmetric, then a Nash stable coalition partition exists[30].

Concluded from Remark 2, the Nash stable coalition partition of the proposed CFG model $\mathcal{G}$ can be proved to exist. Then, we analyze the optimal solution of the stable coalition partition. First, related stable concepts in the game are given as follows.

Definition 7 (Nash Equilibrium [38]): A strategy selection profile $\mathcal{S}^* = (s_1^*, \ldots, s_N^*)$ is a pure strategy NE of game $\mathcal{G} = (\mathcal{N}, \{s_n\}_{n\in\mathcal{N}}, V)$ if and only if no player n can improve its utility by changing its states, i.e.,

$$V_n\big(s_n^*, s_{-n}^*\big) \geq V_n\big(s_n, s_{-n}^*\big) \quad \forall n \in \mathcal{N}\ \forall s_n \in \mathcal{S}_n, s_n \neq s_n^*. \tag{24}$$

Definition 8 (Stable Coalition Partition): A partition Π is said to be *Nash stable* if no player can improve its utility by arbitrarily change its strategy, i.e., if

$$\begin{aligned} &\forall n \in \mathcal{N}, \mathrm{CO}_{c_n} \in \Pi : \big(\mathrm{CO}_{c_n}, \Pi\big) \succeq_n \big(\mathrm{CO}_m, \Pi^*\big) \\ &\qquad \text{for all } \mathrm{CO}_m \in \Pi \cup \{\emptyset\}. \end{aligned} \tag{25}$$

$\Pi^* = (\Pi \backslash \{\mathrm{CO}_m, \mathrm{CO}_{c_n}\} \cup \{\mathrm{CO}_m \cup \{n\}, \mathrm{CO}_{c_n} \backslash \{n\}\})$, then Π is thought to have a stable coalition partition.

Theorem 1: With the preference relation of coalition order, and players take (20) as the utility function, the CFG $\mathcal{G}$ can

be converged to the stable coalition partition. In addition, the optimal solutions of problem $\mathcal{P}$ are one of the stable coalition partitions of $\mathcal{G}$.

Proof: Construct the potential function as $\phi(s_n, s_{-n}) = U_t^{\text{Loc}}(\cdot)$, which represents the total utility from (14). Suppose that for arbitrary UAV n, it changes its strategy from s_n to s'_n in one step move, then the change of the potential function caused by this individual strategy adjustment is calculated as follows:

$$\begin{aligned}&\phi(s_n, s_{-n}) - \phi\left(s'_n, s_{-n}\right)\\ &= U(s_n, s_{-n}) + \sum_{m\in\mathcal{M}\setminus\{c_n, c'_n\}} V(\text{CO}_m, \Pi)\\ &\quad - U_n\left(s'_n, s_{-n}\right) - \sum_{m\in\mathcal{M}\setminus\{c_n, c'_n\}} V(\text{CO}_m, \Pi). \end{aligned} \tag{26}$$

Distinctly, drones which are not in CO_{c_n} and $\text{CO}_{c'_n}$ are completely unaffected by the above strategy adjustment. Therefore, the result of the second and fourth items from (26) is added up to zero. Thus, we have

$$\begin{aligned}\phi(s_n, s_{-n}) - \phi\left(s'_n, s_{-n}\right) = U_n(s_n, s_{-n}) - U_n\left(s'_n, s_{-n}\right)\\ \forall n \in \mathcal{N} \quad \forall \mathcal{S}_n, s'_n \in \mathcal{S}_n. \end{aligned} \tag{27}$$

Then, this game is called exact potential game (EPG) [39] and has at least one Nash equilibrium (NE) point. Suppose that for the NE point (says Π) of $\mathcal{G}$, there exist one player, says $\tilde{n}$, which can improve its utility by change its strategy from $s_{\tilde{n}}$ to $s^*_{\tilde{n}}$. From (8), we conclude that $U_n(s^*_{\tilde{n}}, s_{-\tilde{n}}) > U_n(s_{\tilde{n}}, s_{-\tilde{n}})$, which is contradictory to (24), since $U_n(\cdot)$ is the utility function based on coalition order.

Therefore, for $\mathcal{G}$, given coalition order and $U_n(\cdot)$ as the preference relation and utility function, there exists at least one stable coalition partition Π, i.e., the convergence of $\mathcal{G}$ is guaranteed. Notably, the potential function ϕ prefers the total ranging utility, which guarantees that each player's local utility is involved in the total utility. Hence, the stable coalition partition turns to be the optimal solution of problem $\mathcal{P}$. ■

IV. Cooperative Localization Scheme Design Based on CFG

After constructing and analyzing the stability of the CFG model, this section designs the coalition formation algorithm based on rules given in Section III-D. Further, it builds the cooperative localization scheme based on CFG to perform the clustering-based UAV swarm cooperative localization. The specific flowchart of the scheme is shown in Fig. 3, and each block diagram with a corresponding section.

A. Algorithm Design of CFG Model

Based on the analysis of the stable coalition partition in Section III, this section is introduced to design an algorithm for the proposed CFG model $\mathcal{G}$. The above preference relations and formation rules will be applied in the algorithm design. However, due to the diversity of strategy sets, this kind of optimal selection approach often falls into the trap loop, that is, local optimum.

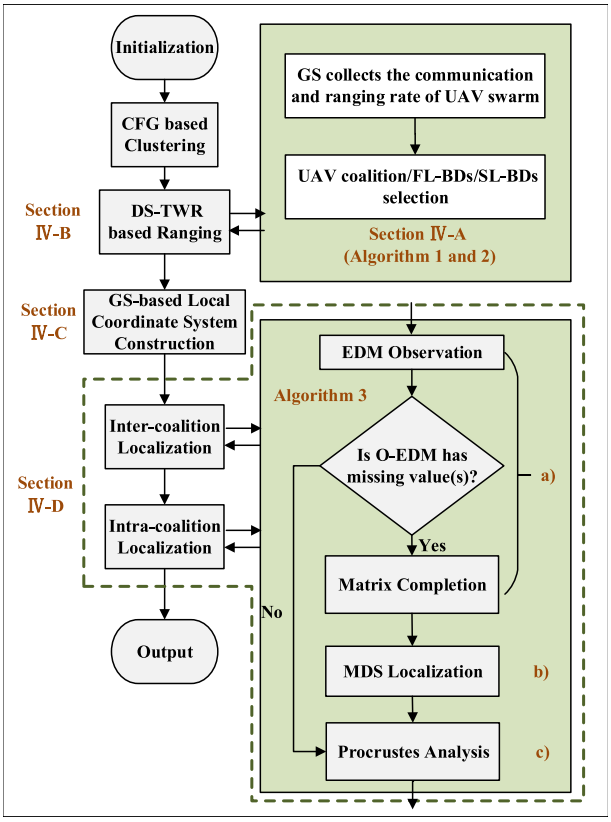

Fig. 3. Cooperative localization scheme design based on CFG.

Motivated by the log-linear learning algorithm designed in [40] and [41], we construct the UAV coalition/FL-BDs/SL-BDs selection algorithm based on coalition order (CSA-CO Algorithm), as shown in Algorithm 1. The algorithm's core is to follow the coalition selection mechanism; according to Theorem 1, it can converge $\mathcal{P}$ in the solution of the problem. Here, β is the learning parameter ($\beta > 0$). The convergence of the log-linear learning algorithm has been proven in [42]. Given the designed utility function, the algorithm can effectively converge to the NE point. By adjusting β, the proposed algorithm can compromise between exploration and selection, which guarantees the effect of convergence and improves the speed of convergence.

According to the proposed algorithm, given two coalitions, says CO_{c_n} and CO_{c_k}, after executing coalition forming/breaking, $\text{CO}^*_{c_n}$ and $\text{CO}^*_{c_k}$ are obtained, then the update probability function is given as follows:

$$\begin{aligned}&\text{Prob}(\Pi(j+1) = \Pi(j)))\\ &= \frac{\exp\{\beta \cdot U(s_n, s_{-n})\}}{\exp\{\beta \cdot U(s_n, s_{-n})\} + \exp\left\{\beta \cdot U\left(s^*_n, s_{-n}\right)\right\}} \end{aligned} \tag{28}$$

$$\text{Prob}\left(\Pi(j+1) = \Pi^*\right) = 1 - P(\Pi(j+1) = \Pi(j)). \tag{29}$$

$U(s_n, s_{-n}) = V(\text{CO}_{c_n}, \Pi) + V(\text{CO}_{c_k}, \Pi)$, $U(s^*_n, s_{-n}) = V(\text{CO}^*_{c_n}, \Pi^*) + V(\text{CO}^*_{c_k}, \Pi^*)$, which are designed based on coalition order. Besides, Algorithm 2 is designed for FL-BDs/SL-BDs selection while coalition selection is determined. This algorithm adopts the best response to complete FL-BDs/SL-BDs selection based on coalition value to obtain the optimal solution.

Algorithm 1: UAV CSA-CO Algorithm

Input : Channel parameters, channel gain $w_{n\to k}$ by (3), $n, k \in \mathcal{N}, n \neq k$, transmit power and positions of GSs and UAV swarm $\{p_\zeta\}_{\zeta\in ref}$, $\{p_n\}_{n\in\mathcal{N}}$, $\{\mathbf{p}_k\}_{k\in ref}$ and $\{\mathbf{p}_n\}_{n\in\mathcal{N}}$.

Initialize: Set an initial coalition partition Π and maximal iteration time J;
Calculate $R^{\text{double}}_{n,k}(\cdot)$ and $R^{\text{loc}}_{n,k}(\cdot)$; // (6), (10)
$j = 1$;
while $j \le J$ *or the stop criterion is met* **do**
  Obtain current coalition partition $\Pi(j)$ and strategy selections $\{s_n(j)\}_{n\in\mathcal{N}}$;
  if ***Coalition Fixed Principle***; // *Switch Rule,* (23)
  then
    Randomly select UAV n and k, $c_n \neq c_k$;
    Switch coalition $c'_n = c_k, c'_k = c_n$;
    Others remain unchanged, i.e. $c_l(j+1) = c_l(j), l \in \mathcal{N}\backslash\{n,k\}$;
    Obtain new coalition partition Π^*;
    $CO^*_{c_n} \leftarrow CO_{c_n} \cup \{k\}\backslash\{n\}$, $CO^*_{c_k} \leftarrow CO_{c_k} \cup \{n\}\backslash\{k\}$
  else if ***Coalition Adapted Principle*** ; // (22)
  then
    Randomly select UAV n;
    Select new coalition i.e. $c'_n = c_k$, $c_n \neq c_k$;
    Others remain unchanged, i.e. $c_l(j+1) = c_l(j), l \in \mathcal{N}\backslash n$;
    Obtain new coalition partition Π^*;
    $CO^*_{c_n} \leftarrow CO_{c_n}\backslash\{n\}$, $CO^*_{c_k} \leftarrow CO_{c_k} \cup \{n\}$
  end
  Enter Algorithm 2 to obtain FL-BDs $ref^{\text{inner}}_{m^*,t}$ and SL-BDs $\{ref^{\text{inner}}_{m,t}\}_{m\in\{c_n,c_k\}}$ i.e. $\{s^*_n\}_{n\in\tilde{CO}}$, where $\tilde{CO} = CO_{c_n} \cup CO_{c_k}$;
  Calculate $V(CO_{c_n}, \Pi)$, $V(CO_{c_k}, \Pi)$, $V(CO^*_{c_n}, \Pi^*)$, $V(CO^*_{c_n}, \Pi^*)$; // (20)
  Calculate $\text{Prob}\big(\Pi(j+1) = \Pi^*\big)$; // (28), (29)
  if $V(CO, \Pi)$ **then**
    $\Pi(j+1) = \Pi^*$;
    $\{s_n(j+1)\}_{n\in\tilde{CO}} = \{s^*_n\}_{n\in\tilde{CO}}$
  else
    $\Pi(j+1) = \Pi(j)$;
    $\{s_n(j+1)\}_{n\in\tilde{CO}} = \{s_n(j)\}_{n\in\tilde{CO}}$
  end
  Others remain unchanged, i.e. $\{s_n(j+1)\}_{n\in\mathcal{N}\backslash\tilde{CO}} = \{s_n(j)\}_{n\in\mathcal{N}\backslash\tilde{CO}}$;
  $j = j + 1$
end
Record total utility of the whole network;

Output : Coalition/FL-BDs/SL-BDs selection of UAV swarm.

Algorithm 2: FL-BDs/SL-BDs Selection Algorithm

Input : UAV set $\tilde{CO} = \{CO_1, \ldots CO_{\tilde{M}}\}$ and strategies $\{s_n\}_{n\in\tilde{CO}}$

Set $u_{\text{FL}} = 0$;
for $m = 1 : \tilde{M}$ **do**
  List all four-tuples in CO_m, denoted as $\tilde{\tilde{\mathcal{N}}}_{4\times\tilde{N}}$;
  Set $u_{\text{SL}} = 0$, $\{a3_n\}_{n\in\tilde{CO}} = 0$, $\{s^*_n\}_{n\in\tilde{CO}} \leftarrow \{s_n\}_{n\in\tilde{CO}}$;
  for $k = 1 : \tilde{N}$; // *Traverse all four-tuples in* CO_m
  do
    $\tilde{\mathcal{N}} \leftarrow \tilde{\tilde{\mathcal{N}}}(:, k)$;
    if $n \in \tilde{\mathcal{N}}$ **then**
      $a2^*_n = 1$
    else
      $a2^*_n = 0$
    end
    Calculate $u^*_{\text{SL}} = \sum_{n\in CO_m} u_n\big(s^*_n, s^*_{-n}\big)$; // (20)
    if $u^*_{SL} > u_{SL}$; // *Best response*
    then
      $u_{\text{SL}} \leftarrow u^*_{\text{SL}}$;
      $\{a2_n\}_{n\in CO_m} \leftarrow \{a2^*_n\}_{n\in CO_m}$
    end
  end
  Update $\{s_n\}_{n\in CO_m}$ from $\{a2_n\}_{n\in CO_m}$;
  Update $\{a3^*_n\}_{n\in CO_m} \leftarrow m = m^*$; // *Suppose* CO_m *contains FL-BDs*
  $\{s^{**}_n\}_{n\in CO_m} \leftarrow \{s_n\}_{n\in CO_m}$;
  Update $\{s^{**}_n\}_{n\in CO_m}$ from $\{a3^*_n\}_{n\in CO_m}$;
  Calculate $u^*_{\text{FL}} = \sum_{n\in CO_m} u_n\big(s^{**}_n, s^{**}_{-n}\big)$; // (20)
  if $u^*_{FL} > u_{FL}$; // *Best response*
  then
    $u_{\text{FL}} \leftarrow u^*_{\text{FL}}$;
    $\{a3_n\}_{n\in CO_m} \leftarrow \{a3^*_n\}_{n\in CO_m}$
  end
end
Update $\{s_n\}_{n\in\tilde{CO}}$ from $\{a3_n\}_{n\in\tilde{CO}}$;

Output : FL-BDs/SL-BDs selection of UAV set $\tilde{CO}$, i.e. $\{s_n\}_{n\in\tilde{CO}}$.

B. DS-TWR-Based Time Slot Design

The operation scheme of DS-TWR is shown in Fig. 4. For instance, in the 4-node network, take UAV 1 as the tag, then UAV 2, UAV 3, and UAV 4 are anchors. The network only needs five measurement frames (sending two frames and receiving three frames) to locate the label and complete the ranging exchange. The propagation time between UAV 1 and UAV $k \in \{2, 3, 4\}$ is calculated as follows:

$$\tau_{1,k} = \frac{\tau_{R_1A} \times \tau_{R_kA} - \tau_{P_1A} \times \tau_{P_kA}}{\tau_{R_1A} + \tau_{R_kA} + \tau_{P_1A} + \tau_{P_kA}}. \tag{30}$$

In that case, the N-node network requires $N(N+1)$ measurement frames in the measurement phase to complete a one-time ranging process. Therefore, under the premise that the synchronization and reporting phase remains unchanged, the duration of all measurement phases is positively correlated with $h(\mathcal{M}_t)$, and the localization frequency is negatively correlated with $h(\mathcal{M}_t)$ in the UAV network.

In [43], we have made some improvements in the time slot design to reduce the number of measurement frames and prolong the network's lifetime. Further, the relevant improving work about measurement frame reducing has been implemented on DW1000, a fully integrated low power, single-chip CMOS radio transceiver IC compliant with the IEEE 802.15.4-2011 UWB standard.

C. Construction of GS-Based Local Coordinate System

As described before, two GSs ref $= \{\text{ref}_1, \text{ref}_2\}$ are settled as beacons to determine coordinate origin, x-axis and y-axis in right-hand system. GSs' altitudes are set to zero, i.e., $h_{\text{ref}_1} = h_{\text{ref}_2} = 0$, thus let the coordinate of GS $\mathbf{p}_{\text{ref}_1}$ be $[0, 0, 0]$, denote the coordinate of ref_2 and drones k as

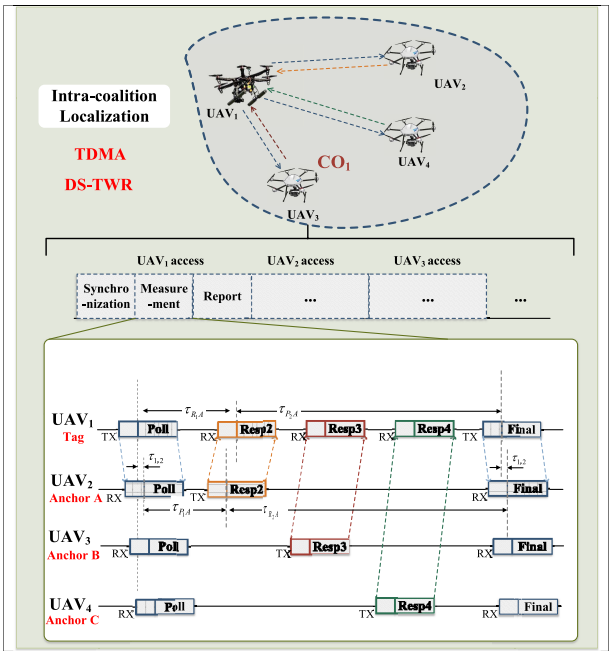

Fig. 4. DS-TWR-based UAV swarm ranging message RX/TX design schematic.

$\mathbf{p}_{\text{ref}_2} = [x_2, 0, h_{\text{ref}_1,\text{ref}_2}]$ and $\mathbf{p}_k = [x_k, y_k, h_{\text{ref}_1,k}]$, respectively, $h_{i,j} = h_j - h_i$, while the altitudes of drones $\{h_k\}_{k\in\mathcal{N}}$ are obtained by their barometers, which can determine the z-axis. Since the ranging measurement between each node $r_{i,j}$ is known, $i, j \in \mathcal{N} \cup ref$, then we have

$$d^2_{\text{ref}_1,\text{ref}_2} = x_2^2 + h^2_{\text{ref}_1,\text{ref}} \tag{31a}$$

$$d^2_{\text{ref}_1,k} = x_k^2 + y_k^2 + h^2_{\text{ref}_1,k} \tag{31b}$$

$$d^2_{\text{ref}_2,k} = \left(x_k - x_{\text{ref}_2}\right)^2 + y_k^2 + \left(h_{\text{ref}_1,k} - h_{\text{ref}_1,\text{ref}_2}\right)^2. \tag{31c}$$

Equations (31a)–(31c) are conventional multivariate equations, which can be directly solved. The absolute position of GS ref_2 and FL-BD k is solved as follows.

D. Relative Localization Method Based on Matrix Completion

After constructing the GS-based local coordinate system and FL-BD localization, the intercoalition localization (SL-BD localization) and the intracoalition localization both adopt a relative localization method based on matrix completion. In intercoalition localization, the BDs are FL-BDs, of which the absolute positions are calculated based on GSs (see Section IV-C). In intracoalition, the BDs are SL-BDs, of which the positions are calculated based on intercoalition localization.

Since four beacons are required for 3-D localization, let the BD set be $\mathcal{N}_2 = \{Ma_1, Ma_2, Ma_3, Ma_4\}, \mathcal{N}_2 \subseteq \text{ref}_t^{inner}$, then the absolute position of BDs is $\mathbf{P}_{Ma} = [\mathbf{p}_{Ma_1}; \mathbf{p}_{Ma_2}; \mathbf{p}_{Ma_3}; \mathbf{p}_{Ma_4}]$. The specific relative localization method based on matrix completion is characterized as follows.

1) EDM Observation and Completion: Suppose N_1 drones need to be located, the set of which is denoted as $\mathcal{N}_1$, then according to DS-TWR described in Section IV-B, the O-EDM $\mathbf{D}_{\text{obs}} \in \mathbb{R}^{N_1\times N_1}$ can be obtained. Analyze the O-EDM and judge whether it lacks ranging value(s); if not, go to step 2); otherwise, the matrix completion method is implemented to fill the missing value(s).

The high dimension of the O-EDM and many missing values bring challenges to the matrix completion. In this article, an alternating LSs (ALSs) [44]-based matrix completion method is adopted to solve the matrix completion problem. The core of the ALS method is matrix factorization (MF). To implement the ALS method, first, transform O-EDM $\mathbf{D}_{\text{obs}}$ into squared Euclidean distance matrix (S-EDM) $\mathbf{D}_{\text{sqd}} \in \mathbb{R}^{N_1\times N_1}$, of which the elements are denoted as $\hat{r}_{n,k} = r^2_{n,k}$; second, reduce the dimension of S-EDM, where S-EDM is decomposed into two low-rank matrices $\mathbf{U}$ and $\mathbf{V} \in \mathbb{R}^{N_1\times j}$

$$\mathbf{D}_{\text{sqd}} \approx \mathbf{U}\mathbf{V}^T. \tag{33}$$

Here, SVD is used to carry out matrix decomposition and obtain $\mathbf{U}$ and $\mathbf{V}$. Finally, the LS optimization is performed alternately on U and V to fill these two low-rank matrices. After several iterations, the method will converge to get an approximate solution

$$\mathbf{U} = \left(\mathbf{V}^T\Lambda\mathbf{V} + \lambda\mathbf{I}\right)^{-1}\mathbf{V}^T\Lambda\mathbf{D}_{\text{sqd}} \tag{34}$$

$$\mathbf{V} = \left(\mathbf{U}^T\Lambda\mathbf{U} + \lambda\mathbf{I}\right)^{-1}\mathbf{U}^T\Lambda\mathbf{D}_{\text{sqd}} \tag{35}$$

where λ represents the predefined regularization parameter, $\mathbf{I} \in \mathbb{R}^{N_1\times N_1}$ is the identity matrix, and $\Lambda \in \mathbb{R}^{N_1\times N_1}$ is a diagonal matrix, representing weighting factor for evaluating the ranging quality, which is generally assigned as the reciprocal of the ranging variance $\sigma^{-2}_{n,k}$. Finally, the filled matrix $\hat{\mathbf{D}} \in \mathbb{R}^{N_1\times N_1}$ is obtained through (33)

2) MDS Relative Localization for Relative Maps Acquisition: First, calculate the centralized inner product matrix as follows:

$$\mathbf{H} = -\frac{1}{2}\cdot\mathbf{J}\hat{\mathbf{D}}\mathbf{J} \tag{36}$$

where $\mathbf{J} = \mathbf{I}_{N_1} - \mathbf{1}_{N_1}\mathbf{1}^T_{N_1}/N_1$. Then, carry out SVD on the matrix $\mathbf{H}$

$$[\mathbf{U}, \mathbf{S}, \mathbf{V}] = \text{SVD}(\mathbf{H}) \tag{37}$$

$$\mathbf{p}_{\text{ref}_2} = \left[\sqrt{d^2_{\text{ref}_1,\text{ref}_2} - h^2_{\text{ref}_1,\text{ref}_2}}, 0, h_{\text{ref}_1,\text{ref}_2}\right] \tag{32a}$$

$$\mathbf{p}_k = \left[\frac{1}{2}\frac{\sqrt{d^2_{\text{ref}_1,k} - d^2_{\text{ref}_2,k} + h^2_{\text{ref}_2,k} - h^2_{\text{ref}_1,k} + x^2_{\text{ref}_2}}}{x_{\text{ref}_2}}, \sqrt{d^2_{\text{ref}_1,k} - h^2_{\text{ref}_1,k} + x_k^2}, h_{\text{ref}_1,k}\right] \tag{32b}$$

TABLE I
TABLE OF SIMULATION PARAMETER SETTING

Parameter Name	Parameter Setting	Parameter Name	Parameter Setting
UAV amount	$N = 40 \sim 100$	Channel background noise	$N_0 = -174dB/Hz$
Coalition amount	$M = 4 \sim 10$	Channel bandwidth	$B = 500MHz$
UAV transmit power	$p_n = 15\text{dbm}$	Path fading factor	$\alpha = 2$
Border length	$L_{\text{lg}} = 4km \sim 6km$	Boltzmann coefficient	$\beta = 5 \sim 200$
Border width	$L_{\text{wd}} = 4km \sim 6km$	Regularization parameter	$\gamma = 0.1$
Border height	$L_{\text{he}} = 2km \sim 3km$	Demodulation threshold	$\eta_0 = 1$
Diagonal matrix	$\mathbf{\Lambda} = \text{diag}\underbrace{\{0.1, \ldots, 0.1\}}_{N_1}$	Fading coefficient variance	$\eta_{dB} = 12dB$

where $\mathbf{H} = \mathbf{USV}^T$. Next, the relative map is calculated as follows:

$$\mathbf{P}_{re} = \hat{\mathbf{X}}(1{:}3, :) \tag{38}$$

and $\hat{\mathbf{X}} = \mathbf{VS}^{(1/2)}$, of which the first 3-D values are chosen as the result of 3-D localization.

3) Procrustes Analysis for Coordinate Transformation: The positions of the drones in the relative map $\mathbf{P}_{re}$ can be mapped to their absolute positions through a linear transformation. Since the positions of the beacons are calculated as

$$\mathbf{P}_{\text{ref}} = [\mathbf{P}_{re}(:, Ma_1); \mathbf{P}_{re}(:, Ma_2); \mathbf{P}_{re}(:, Ma_3); \mathbf{P}_{re}(:, Ma_4)]. \tag{39}$$

Procrustes analysis is adopted to solve the linear transformation from $\mathbf{P}_{\text{ref}}$ to $\mathbf{P}_{Ma}$. Specifically, through continuous iteration, the LS method is used to find the transformation relation from the current shape ($\mathbf{P}_{\text{ref}}$) to the standard shape ($\mathbf{P}_{Ma}$). The affine change boils down to a structure array, which contains three parameters: 1) $\mathbf{T}$ (orthogonal rotation transformation); 2) b (scale transformation); and 3) $\mathbf{c}$ (translation transformation), which makes

$$\{b, \mathbf{T}, \mathbf{c}\} \leftarrow \mathbf{P}_{Ma} = b \cdot \mathbf{P}_{\text{ref}} \cdot \mathbf{T} + \mathbf{c}. \tag{40}$$

Since it is not the innovative work of this article, the description of the Procrustes analysis is omitted here. Related work and codes (MATLAB/Python) are available online. Therefore, based on these transformation parameters, the relative positioning result of MDS can be converted into the absolute positions

$$\{\mathbf{p}_n\}_{n \in \mathcal{N}_1} = b \cdot \mathbf{P}_{re} \cdot \mathbf{T} + \mathbf{c}. \tag{41}$$

Algorithm 3 shows the relative localization process of this section.

Algorithm 3: UAV Swarm Relative Localization Algorithm Based on Matrix Completion

Input: UAV swarm's coalition partition Π; FL-BD set $ref_{m^*}^{\text{inner}}$ and SL-BD set ref_m^{inner} from Algorithm 1; Channel parameters; Corresponding O-EDMs for every coalition

// ***FL-BDs Localization***
Calculate and obtain the "absolute positions" of the FL-BDs $\{\mathbf{p}_k\}_{k \in ref_{m^*}^{\text{inner}}}$; // (31) *and* (32)
// $m = 0 \rightarrow$ ***Inter-coalition/SL-BDs Localization***
// $m > 0 \rightarrow$ ***Intra-coalition Localization***
for $m = 0$ *to* M **do**
  Obtain O-EDMs of FL-BD set $ref_{m^*}^{\text{inner}}$ and SL-BD set ref_m^{inner}, described as $\mathbf{D}_{\text{obs}_m}$, $\mathbf{D}_{\text{sqd}_m} \leftarrow \mathbf{D}_{\text{obs}_m}$;
  if $\mathbf{D}_{obs_m}$ *has missing value(s)* **then**
    $\hat{\mathbf{D}}_m \leftarrow \mathbf{D}_{\text{sqd}_m}$; // *Matrix Completion,* (33)–(35)
  else
    $\hat{\mathbf{D}}_m \leftarrow \mathbf{D}_{\text{obs}_m}$
  end
  $\mathbf{P}_{re} \leftarrow \hat{\mathbf{D}}_m$; // *Relative Map Acquisition,* (36)–(38)
  Choose beacons $\mathbf{P}_{ref}$; // (39)
  Calculate transformation relations $\{b, \mathbf{T}, \mathbf{c}\}$ from $\mathbf{P}_{Ma} \leftarrow \mathbf{P}_{ref}$; // (40)
  $\{\mathbf{p}_n\}_{n \in \mathcal{N}_1} \leftarrow \mathbf{P}_{re}$; // *"Absolute Positions" Mapping,* (41)
end
Record performance metrics;
Output: Relative Localization Results of UAV swarm $\{\mathbf{p}_n\}_{n \in \mathcal{N}}$.

V. SIMULATION RESULTS AND DISCUSSION

In this section, we carry out simulations to verify the convergence and localization performance of the proposed cooperative localization scheme to confirm the validity of the proposed ranging-based cooperative localization CFG model. MATLAB R2020b is used as the simulation tool.

A. Simulation Environment

The mission area is located in a 3-D space ($L_{\text{lg}} \times L_{\text{wd}} \times L_{\text{he}}$), in which drones are randomly deployed. Set the position of GSs as $\mathbf{p}_{\text{ref}_1} = [0, 0, 0](\text{m})$ and $\mathbf{p}_{\text{ref}_1} = [500, 0, 0](\text{m})$. Consider the fading characteristics of the wireless channel and establish the lognormal fading model [45]. From (3), we can see that the channel gain is related to the path fading factor and the instantaneous fading coefficient ε_t. ε_t is a Gaussian variable whose mean is zero and variance is η, and $\eta = 0.1 \times \log(10) \times \eta_{dB}$. Specific settings of other simulation parameters are set as follows.

The variables in Table I are the parameters used for performance analysis in the simulation. Unless otherwise specified, other parameters will be tailored according to the table. It can be concluded from (14) that the amount of coalition and coalition members will significantly affect

localization performance. The proposed UAV swarm cooperative localization scheme based on CFG performs coalition selection, then executes relative localization. In order to compare the robustness and effectiveness of the scheme in different scenarios, the CSA-CO algorithm with four coalition amounts (abbreviated as 4 CA-CFG, the same below), six coalition amounts (6 CA-CFG), eight coalition amounts (8 CA-CFG), and ten coalition amount (10 CA-CFG) are proposed. Comparison algorithms are presented, where coalition amount and members are both preset and fixed based on the initial distances among drones (abbreviated as 4 CA-FIX, 6 CA-FIX, 8 CA-FIX, and 10 CA-FIX with different coalition amounts). In addition, a global localization comparison algorithm is also introduced, where the UAV network obtains ranging information of all drones in a unified manner. Since our proposed CFG scheme includes a matrix completion method, comparison algorithms are presented with no matrix completion method (abbreviated as MDS-MAP without MC). The main difference between these algorithms is that the O-EDMs after coalition formation are different. All algorithms carry out relative localization based on matrix completion and output the absolute positions of the UAV swarm. In order to avoid the contingency of the algorithms, 100 independent algorithm reruns were performed, each of which randomly generates network topology; that is, the positions of the UAV swarm in the mission area are randomly generated each time the average results are finally taken.

Next, the performance metrics are introduced to make an intuitive and effective presentation of localization performance, which serves to draw conclusions. The performance metrics are described as follows.

1) Root-Mean-Squared Error: Root-mean-squared error (RMSE) is one of the most common indexes to measure the accuracy of variables. It is used in localization performance analysis to calculate the deviation between the localization measurement results $\mathbf{p}_n$ and the true position value $\hat{\mathbf{p}}_n$, i.e.,

$$\text{RMSE (m)} = \sqrt{\frac{1}{N}\sum_{n=1}^{N}\left\|\mathbf{p}_n - \hat{\mathbf{p}}_n\right\|^2}. \tag{42}$$

2) Localization Success Rate: An important issue about performance analysis is that packet loss still exists when facing the circumstance that part of drones is relatively far. In that case, both clustering and matrix filling methods cannot effectively alleviate the ranging correction error, resulting in colossal localization offset for drones. Given that RMSE cannot well characterize the performance, localization success rate (LocSR) is adopted to characterize the localization performance of different algorithms, which are

$$\text{LocSR (\%)} = \frac{\text{Card}(\mathcal{N}_{\text{succ}})}{\text{Card}(\mathcal{N})} \times 100\% \tag{43}$$

where $\mathcal{N}_{\text{succ}} = \{n \in \mathcal{N} | \|\mathbf{p}_n - \hat{\mathbf{p}}_n\| < e_{\text{th}}\}$, e_{th}(m) represents the maximum error to determine a successful localization. Obviously, the numerical value of the LocSR directly indicates the strength of localization performance.

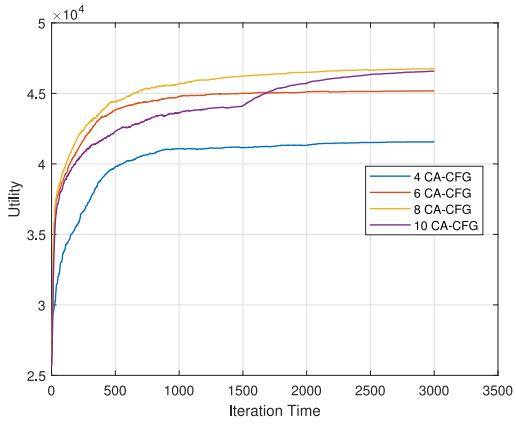

Fig. 5. Convergence curve of the whole network's utility $U_t^{\text{Loc}}(\cdot)$ with iteration times (Border: 5000 m × 5000 m × 2500 m).

3) Ranging Message Amount: From Sections II-B3 and IV-B, the localization frequency $\text{fre}(\mathcal{M}_t)$ is in anti-correlation relation with $h(\mathcal{M}_t)$. We denote $h(\mathcal{M}_t)$ as ranging message amount (RMA) from (15). The larger the RMA, the more ranging messages and the longer the time required to complete a localization. Simulation results are shown as follows.

B. Convergence Performance for Coalition Formation

According to Theorem 1, the proposed CFG G has at least one stable coalition partition (i.e., formation) with the coalition order. Therefore, the convergence performance is analyzed to verify the effectiveness of the proposed UAV CSA-CO algorithm.

Consider a mission area with 5000 m × 5000 m × 2500 m border where 50 drones are deployed. Channel parameters and other scenario conditions are given according to Table I. Fig. 5 shows the convergence curve of the total utility of the UAV network $U_t^{\text{Loc}}(\cdot)$ under the CSA-CO algorithm considering different coalition amounts (100 reruns and averaged). Notably, confidence interval analysis of multiple reruns shows that the variance of the convergence performance of the curve is relatively small, which is consistent with the statement that the CSA-CO algorithm can effectively converge the proposed CFG model to the stable state. In addition, the final convergence values of utility under different algorithms are not the same, which is supported by (14), where the coalition and coalition members result in different cooperative relations. Given the above condition, the total utility under 8 CA-CFG and 10 CA-CFG is nearly the same, while under 6 CS-CFG and 4 CA-CFG is worse. Thus, identical conclusions were obtained that the utility of the UAV network is related to the amount of coalition and coalition members.

As shown in Figs. 6 and 7 (take 4 CA-CFG and 6 CA-CFG, for instance), each drone performs the strategy selection according to the utility function, resulting in a change of drone amount in each coalition. At the beginning of the iteration, drones tend to explore the available coalitions that bring high payoff to them due to the small learning coefficient. In

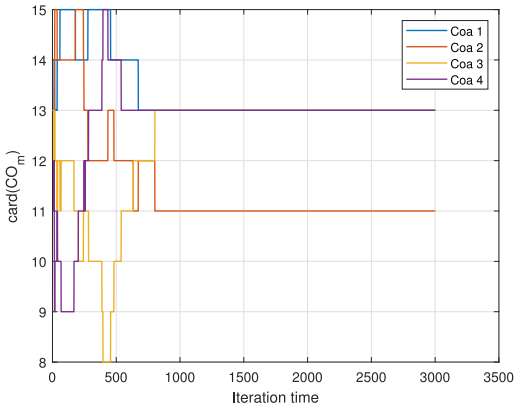

Fig. 6. Convergence curve of the drone amount belonging to each coalition $CO_m, m \in \mathcal{M}$ with iteration times (Border: 5000 m × 5000 m × 2500 m, $\text{card}(CO_m) = 4$.

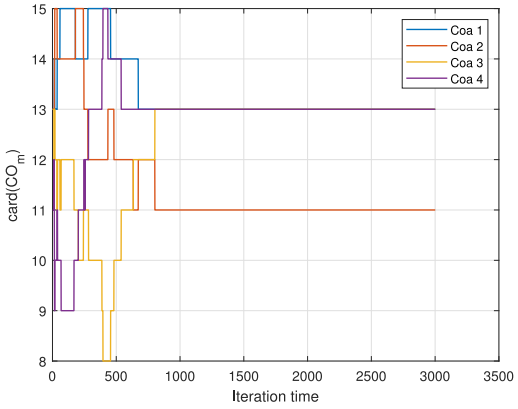

Fig. 7. Convergence curve of the drone amount belonging to each coalition $CO_m, m \in \mathcal{M}$ with iteration times (Border: 5000 m × 5000 m × 2500 m, $\text{card}(CO_m) = 6$.

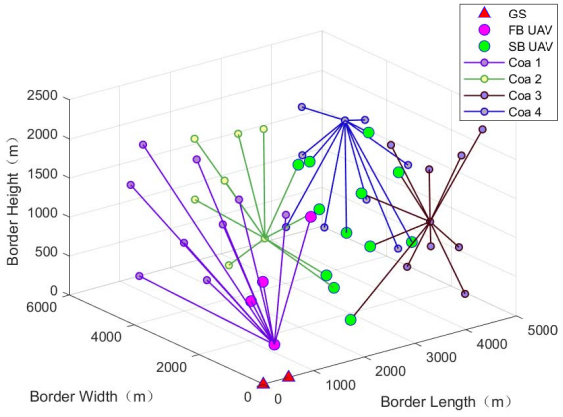

Fig. 8. Schematic of coalition formation with four CA-CFG algorithm converges (3-D view, Border: 5000 m × 5000 m × 2500 m, $M = 4$).

the later iteration stage, the proposed algorithm finally converged to NE, that is, the stable coalition partition, where the drone amount in each coalition remains unchanged. The results illustrate that the strategy selection gradually approached the steady state, and the learning coefficient adjustment also makes the drones more inclined to the optimal selection.

To better understand the clustering effect presented by the proposed algorithms, Figs. 8 and 9 present a schematic of the

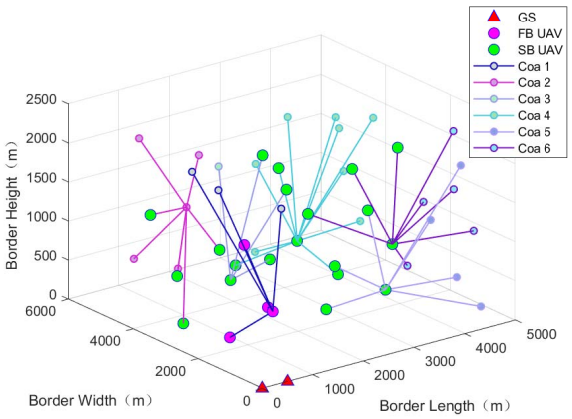

Fig. 9. Schematic of coalition formation with four CA-CFG algorithm converges (3-D view, Border: 5000 m × 5000 m × 2500 m, $M = 6$).

distribution of swarm and coalition formation (clustering) in the 3-D mission area. In these figures, the red triangle represents GSs, the rose and green circle represent FL-BDs and SL-BDs, respectively, and the smaller circles in other colors represent coalition members. A solid line connects each coalition member, and the convergence point of the connection indicates the coalition head. Drones form coalitions (clusters) with distance priority. The number of coalition members under 4CA-CFG is 13, 11, 13, and 13, respectively, and the number of members under 6CA-CFG is 7, 9, 5, 12, 8, and 9, respectively. This result agrees with the coalition selection convergence shown in the figure above. The CFG-based algorithms improve the localization performance by adjusting the coalition selection of the UAV swarm, while the contrast algorithms do not.

Hence, the convergence simulations of the proposed algorithm verify the existence of the stable coalition formation.

C. Performance Elevation for Localization

In order to profoundly investigate the improvement of the proposed algorithms (4/6/8/10 CA-CFG), contrast algorithms (4/6/8/10 CA-FIX and global localization) are adopted in CFG-based clustering, where localization performance metrics are analyzed through relative localization, as described in Section V. The related simulation results are shown as follows.

1) Performance Comparison Considering Border Size: Set UAV amount N as 50, Figs. 10 and 11, respectively, show the LocSR and RMSE of the UAV network considering border size under the proposed algorithms and the comparison algorithms. The border size is numerically equal to border length L_{lg}, border width L_{wd}, and half of the border height $L_{\text{he}}/2$.

Notably, when the border size is less than 4500 m, for the proposed CFG algorithms, the LocSR approaches 100%, and the RMSE is relatively low (nearly 10-m level). In contrast, the LocSR and RMSE of the comparison algorithms are worse, RMSE of comparison algorithms even directly increases to the kilometer level. The analyses are as follows. Global localization does not use clustering and is most seriously affected by long-distance packet loss, which makes the localization effect very poor. CA-FIX algorithms execute clustering simply

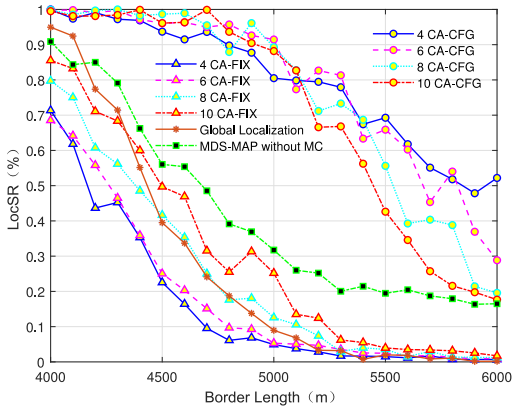

Fig. 10. Performance comparison of LocSR (%) under different algorithms considering border size (UAV amount: $N = 50$).

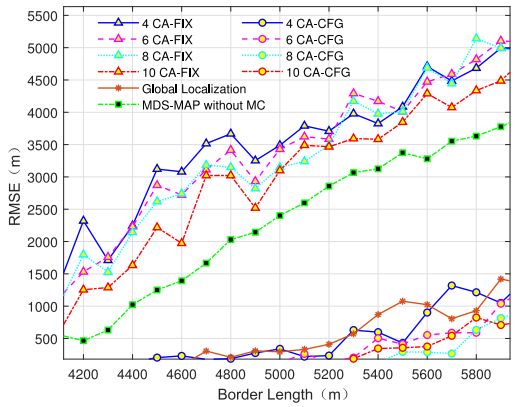

Fig. 11. Performance comparison of RMSE (m) under different algorithms considering border size (UAV amount: $N = 50$).

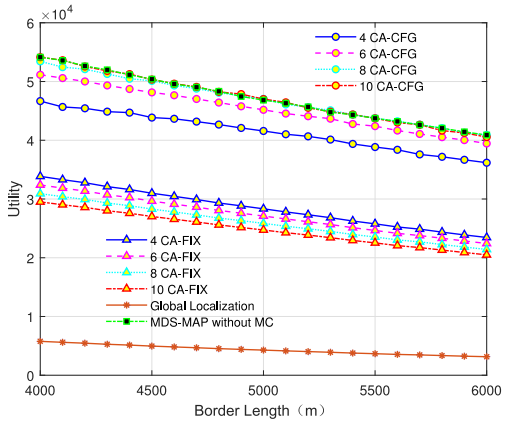

Fig. 12. Performance comparison of UAV network's utility $U_t^{\mathrm{Loc}}(\cdot)$ under different algorithms considering border size (UAV amount: $N = 50$).

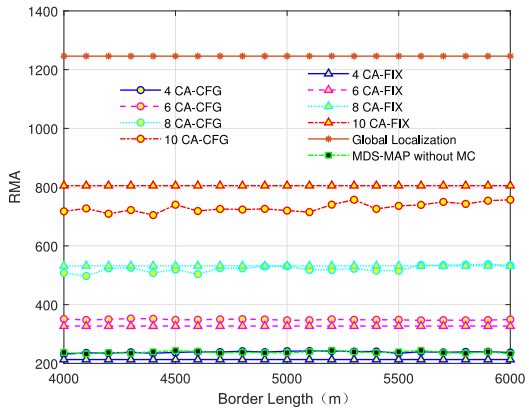

Fig. 13. Performance comparison of RMA $h(\mathcal{M}_t)$ under different algorithms considering border size (UAV amount: $N = 50$).

relying on the Euclidean distance while ignoring the cooperative relationships among drones and not considering global relative localization's utility. The MDS-MAP without MC algorithm achieves good clustering through the proposed CFG scheme but does not use the matrix completion scheme to modify the O-EDM. In addition, we have concluded from the CA-CFG and CA-FIX algorithms result that the different coalition (clusters) amounts will also affect the localization effect. This is because the coalition amounts significantly affect the selections of FL-BDs and SL-BDs, thereby affecting the localization accuracy of different coalitions.

As the border size increases, the LocSR of all algorithms decreases, and the RMSE will also increase. The result is in line with the actual perception. When the border size exceeds 5000 m, the proposed CA-CFG algorithms cannot solve the packet loss caused by long-distance ranging but still have made a very noticeable localization performance compared with comparison algorithms.

Given the simulation parameters as described above, Figs. 12 and 13, respectively, show the UAV network's total utility and RMA considering border size under the proposed algorithms and the contrast algorithms. From Fig. 12, as the border size increases, the utility of all algorithms will decrease. The decrease is that drones are set to fill the entire mission area, and a larger border size of the mission area will lead to a longer distance among drones, causing the ranging rate to drop. Furthermore, the proposed CA-CFG algorithms achieve better performance than the comparison algorithms, which indicates that the proposed algorithms perform better coalition formation (clustering) for UAV swarm; thus, ranging packet loss is effectively reduced. These results are in good consistent with the problem goal of the proposed CFG model. From Fig. 13, we can see that the RMA of the proposed algorithms and the contrast algorithms under the same coalition amount are slightly different. The results demonstrate that drones select coalition based on the utility function in the proposed algorithms, but the number of coalition members will fluctuate since the coalition amount is fixed. According to (15), changes in the number of coalition members will not significantly affect RMA. From the results we have obtained, one can conclude that the proposed model can optimize the problem target by adjusting the UAV coalition selection.

In order to further analyze the relationships between the simulation results and coalition amount, we averaged the various results of all algorithms and listed them in the table. As shown in Table II, under the same coalition amount, the increase of the total utility corresponds to the decrease of RMSE and the increase of LocSR. It tests the proposed model's effectiveness and shows that

TABLE II
STATISTICAL ANALYSIS CONSIDERING BORDER SIZE

Algorithm	Utility	up↑(%)	RMA	RMSE (m)	LocSR (%)	up↑(%)
4 CA-FIX	2.84×10^4	-	213	3448.91	16.20	-
4 CA-CFG	4.15×10^4	45.7	238.2	459.35	79.53	63.33
6 CA-FIX	2.72×10^4	-	327	3335.07	18.12	-
6 CA-CFG	4.53×10^4	66.3	348.9	295.48	78.99	60.87
8 CA-FIX	2.60×10^4	-	532	3256.58	24.16	-
8 CA-CFG	4.70×10^4	80.8	521.9	191.23	74.94	50.78
10 CA-FIX	2.48×10^4	-	805	2929.59	30.20	-
10 CA-CFG	4.71×10^4	89.8	731.1	223.45	71.09	40.89

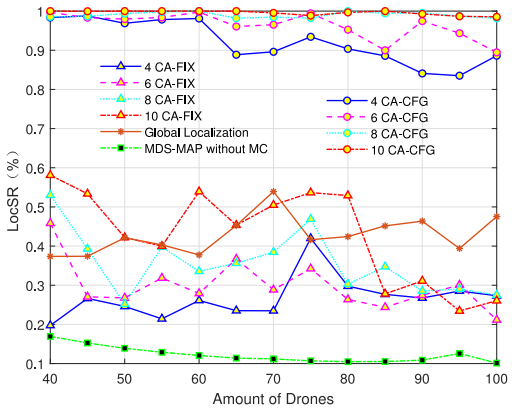

Fig. 14. Performance comparison of LocSR (%) under different algorithms considering UAV amount (Border: 5000 m × 5000 m × 2500 m).

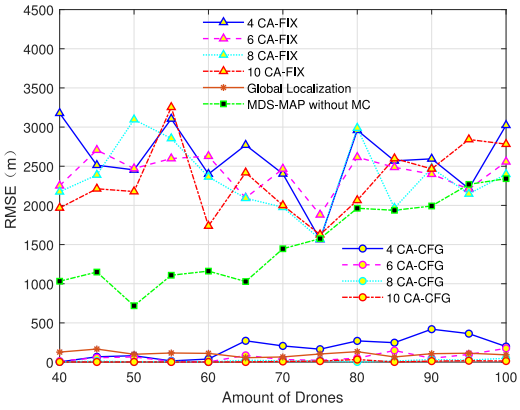

Fig. 15. Performance comparison of RMSE (m) under different algorithms considering UAV amount (Border: 5000 m × 5000 m × 2500 m).

TABLE III
STATISTICAL ANALYSIS CONSIDERING UAV AMOUNT

Algorithm	Utility	up↑(%)	RMA	RMSE (m)	LocSR (%)	up↑(%)
4 CA-FIX	6.50×10^4	-	296.2	2596.0	26.73	-
4 CA-CFG	7.51×10^4	27.5	330.2	180.3	92.08	65.34
6 CA-FIX	6.36×10^4	-	362.6	2412.7	29.89	-
6 CA-CFG	8.14×10^4	47.4	402.4	61.5	96.36	66.46
8 CA-FIX	6.20×10^4	-	551.2	2345.5	35.53	-
8 CA-CFG	9.29×10^4	60.5	576.2	15.7	99.01	63.48
10 CA-FIX	6.11×10^4	-	807.8	2319.1	42.95	-
10 CA-CFG	9.69×10^4	70.9	793.1	8.0	99.58	56.63

the proposed method can effectively improve the localization performance without nearly changing the localization frequency. However, when comparing CA-CFG algorithms with different coalition amount, the total utility does not show a certain linear relationship with RMSE and LocSR. It is because coalition amount determines the upper limit of the ranging rate of the entire network. Hence, the utility of the algorithms considering different coalition amount cannot be directly compared. It shows that further work need to be explored, where richer physical parameter should be utilized to characterize the localization performance, so as to achieve adaptive coalition formation, i.e., adaptively adjust the amount of coalitions and the amount of coalition members according to the utility function.

Besides, it is worthwhile mentioning that the more of the coalition amount, the better the localization performance of the proposed CFG algorithm can achieve. Our analysis believes that more coalition amount reduces the distance among intra-coalition drones while making no effect of intercoalition drones to better avoid the ranging packet loss. Once again, we conclude from the table that when considering the change of border size, the proposed CA-CFG algorithms achieve better performance than the comparison algorithms.

2) Performance Comparison Considering UAV Amount: To further explore the simulation results, we consider the localization performance comparison of the UAV network with the UAV amount between the proposed and contrast algorithms. The mission area is located in a 5000 m × 5000 m × 2500 m 3-D space, and other parameters are also taken from Table I. Performance comparison results of LocSR and RMSE are shown in Figs. 14 and 15, respectively.

The advantages of the proposed algorithms over the comparison algorithm mentioned in Section V-C1 will not be repeated. As the UAV amount increases, the LocSR of some proposed algorithms (4/6 CA-CFG) has declined to a certain extent, while the corresponding RMSE has also increased. We analyze that too few coalitions lead to an increase in the accumulation of localization errors. The increase in coalition amounts makes the more significant number of drones not significantly affect the propagation of localization errors. Therefore, we conclude that the UAV coalitions are formed to prevent the loss of ranging packets to achieve optimal localization performance directly. Likewise, with simulation results and the number of coalitions, we averaged the various index parameters of all algorithms to analyze the relationships among them further, as shown in Table III. From the results we have obtained, one can conclude that as the border size increased to a certain distance, the two-level UAV clustering cannot solve the problem of packet loss, thus making long-distance localization a very promising challenge. This article performs the relative localization based on GSs, suppose part of drones can obtain GNSS information, then the CFG-based scheme is still available.

Therefore, we come to the conclusion that the proposed CA-CFG algorithms make full use of the existing ranging information, fully utilize the ranging information of inter/intra-coalition localization, and finally improve the localization accuracy of the clustering-based UAV swarm localization.

In addition, CFG games have great potential as a tool for UAV swarm clustering based on mission requirements. Considering that multilevel localization is an excellent theoretical basis and algorithm guidance for long-distance

ranging, overlapping BDs between clusters, overlapping coalition formation (OCF) games can be adopted for the system model to achieve better localization performance.

VI. Conclusion

This article investigates a cooperative relative localization scheme for UAV swarm based on the CFG. The proposed UAV swarm localization problem is transformed into a two-level framework: inter/intra-cluster localization. In order to investigate the tradeoff between intracluster cooperation and intercluster packet loss, the clustering-based problem is constructed as a CFG model. Given the designed coalition value, preference relation, and coalition formation principles, we prove that the stable coalition partition of the CFG model exists. Employing DS-TWR and GS-based local coordinate systems, the CFG-based algorithms are developed. Simulation results show that the proposed CFG algorithms shorten the ranging time compared with global localization and achieve better localization performance (localization error and success rate) than contrast algorithms. This work should thus have great potential to improve PNT capabilities for UAV swarm in GNSS-denied scenarios. Combined with game theory and learning algorithms, there is still a lot of research potential in relative localization, especially in long-distance localization.

References

[1] Y. Zeng, R. Zhang, and T. J. Lim, "Wireless communications with unmanned aerial vehicles: Opportunities and challenges," *IEEE Commun. Mag.*, vol. 54, no. 5, pp. 36–42, May 2016.

[2] J. Mortier, G. Pages, and J. Vila-Valls, "Robust TOA-based UAS navigation under model mismatch in GNSS-denied harsh environments," *Remote Sens.*, vol. 12, no. 18, p. 2928, 2020.

[3] S. Minaeian, J. Liu, and Y.-J. Son, "Vision-based target detection and localization via a team of cooperative UAV and UGVs," *IEEE Trans. Syst., Man, Cybern., Syst.*, vol. 46, no. 7, pp. 1005–1016, Jul. 2016.

[4] G. Wu, "UAV-based interference source localization: A multimodal Q-learning approach," *IEEE Access*, vol. 7, pp. 137982–137991, 2019.

[5] Y. Liu, Y. Wang, J. Wang, and Y. Shen, "Distributed 3D relative localization of UAVs," *IEEE Trans. Veh. Technol.*, vol. 69, no. 10, pp. 11756–11770, Oct. 2020.

[6] M. Y. Arafat and S. Moh, "Localization and clustering based on swarm intelligence in UAV networks for emergency communications," *IEEE Internet Things J.*, vol. 6, no. 5, pp. 8958–8976, Oct. 2019.

[7] L. Ruan *et al.*, "Energy-efficient multi-UAV coverage deployment in UAV networks: A game-theoretic framework," *China Commun.*, vol. 15, no. 10, pp. 194–209, Oct. 2018.

[8] N. Qi, N. I. Miridakis, M. Xiao, T. A. Tsiftsis, R. Yao, and S. Jin, "Traffic-aware two-stage queueing communication networks: Queue analysis and energy saving," *IEEE Trans. Commun.*, vol. 68, no. 8, pp. 4919–4932, Aug. 2020.

[9] Y. Shang and W. Ruml, "Improved MDS-based localization," in *Proc. IEEE INFOCOM*, vol. 4. Hongkong, China, 2004, pp. 2640–2651.

[10] W. Jiang, C. Xu, L. Pei, and W. Yu, "Multidimensional scaling-based TDOA localization scheme using an auxiliary line," *IEEE Signal Process. Lett.*, vol. 23, no. 4, pp. 546–550, Apr. 2016.

[11] A. Ghods and G. Abreu, "Complex-domain super MDS: A new framework for wireless localization with hybrid information," *IEEE Trans. Wireless Commun.*, vol. 17, no. 11, pp. 7364–7378, Nov. 2018.

[12] M. Hamaoui, "Non-iterative mds method for collaborative network localization with sparse range and pointing measurements," *IEEE Trans. Signal Process.*, vol. 67, no. 3, pp. 568–578, Feb. 2019.

[13] R. Chen, B. Yang, and W. Zhang, "Distributed and collaborative localization for swarming UAVs," *IEEE Internet Things J.*, vol. 8, no. 6, pp. 5062–5074, Mar. 2021.

[14] N. Saeed and H. Nam, "Cluster based multidimensional scaling for irregular cognitive radio networks localization," *IEEE Trans. Signal Process.*, vol. 64, no. 10, pp. 2649–2659, May 2016.

[15] H. Zou, B. Huang, X. Lu, H. Jiang, and L. Xie, "A robust indoor positioning system based on the procrustes analysis and weighted extreme learning machine," *IEEE Trans. Wireless Commun.*, vol. 15, no. 2, pp. 1252–1266, Feb. 2016.

[16] A. Singh and S. Verma, "Graph laplacian regularization with procrustes analysis for sensor node localization," *IEEE Sensors J.*, vol. 17, no. 16, pp. 5367–5376, Aug. 2017.

[17] A. P. Behera, A. Singh, S. Verma, and M. Kumar, "Manifold learning with localized procrustes analysis based WSN localization," *IEEE Sens. Lett.*, vol. 4, no. 10, pp. 1–4, Oct. 2020.

[18] Y. Shang, W. Ruml, Y. Zhang, and M. P. J. Fromherz, "Localization from mere connectivity," in *Proc. 4th ACM Int. Symp. Mobile Ad Hoc Netw. Comput.*, 2003, pp. 201–212.

[19] N. Saeed, H. Nam, T. Y. Al-Naffouri, and M.-S. Alouini, "A state-of-the-art survey on multidimensional scaling-based localization techniques," *IEEE Commun. Surveys Tuts.*, vol. 21, no. 4, pp. 3565–3583, 4th Quart., 2019.

[20] H. Zhang, Y. Liu, and H. Lei, "Localization from incomplete euclidean distance matrix: Performance analysis for the SVD–MDS approach," *IEEE Trans. Signal Process.*, vol. 67, no. 8, pp. 2196–2209, Apr. 2019.

[21] W. Saad, Z. Han, A. Hjorungnes, D. Niyato, and E. Hossain, "Coalition formation games for distributed cooperation among roadside units in vehicular networks," *IEEE J. Sel. Areas Commun.*, vol. 29, no. 1, pp. 48–60, Jan. 2011.

[22] W. Saad, Z. Han, R. Zheng, A. Hjorungnes, T. Basar, and H. V. Poor, "Coalitional games in partition form for joint spectrum sensing and access in cognitive radio networks," *IEEE J. Sel. Topics Signal Process.*, vol. 6, no. 2, pp. 195–209, Apr. 2012.

[23] W. Saad, Z. Han, M. Debbah, A. Hjorungnes, and T. Basar, "Coalitional game theory for communication networks," *IEEE Signal Process. Mag.*, vol. 26, no. 5, pp. 77–97, Sep. 2009. [Online]. Available: http://dx.doi.org/10.1109/MSP.2009.000000

[24] D. Neirynck, E. Luk, and M. McLaughlin, "An alternative double-sided two-way ranging method," in *Proc. 13th Workshop Position. Navigation Commun. (WPNC)*, 2016, pp. 1–4.

[25] N. Qi, M. Xiao, T. A. Tsiftsis, R. Yao, and S. Mumtaz, "Energy efficient two-tier network-coded relaying systems considering processing energy costs," *IEEE Trans. Veh. Technol.*, vol. 68, no. 1, pp. 999–1003, Jan. 2019.

[26] Q. Wu, Y. Xu, J. Wang, L. Shen, J. Zheng, and A. Anpalagan, "Distributed channel selection in time-varying radio environment: Interference mitigation game with uncoupled stochastic learning," *IEEE Trans. Veh. Technol.*, vol. 62, no. 9, pp. 4524–4538, Nov. 2013. [Online]. Available: http://dx.doi.org/10.1109/TVT.2013.2269152

[27] J. V. Neumann and O. Morgenstern, *Theory of Games and Economic Behavior: 60th Anniversary Commemorative Edition*. Princeton, NJ, USA: Princeton Univ.Press, 1953.

[28] R. Aumann and B. Peleg, "Von Neumann-Morgenstern solutions to cooperative games without side payments," *Bull. Trans. Amer. Math. Soc.*, vol. 66, no. 3, pp. 173–179, 1960.

[29] J. Hamilton, "Game theory: Analysis of conflict, by Myerson, R. B., Cambridge: Harvard University Press," *Manage. Decis. Econ.*, vol. 13, no. 4, p. 369, 1992. [Online]. Available: https://onlinelibrary.wiley.com/doi/abs/10.1002/mde.4090130412

[30] A. Bogomolnaia and M. O. Jackson, "The stability of hedonic coalition structures," *Games Econ. Behav.*, vol. 38, no. 2, pp. 201–230, 2002. [Online]. Available: https://www.sciencedirect.com/science/article/pii/S0899825601908772

[31] S. Banerjee, H. Konishi, and T. Sonmez, "Core in a simple coalition formation game," *Social Choice Welfare*, vol. 18, no. 1, pp. 135–153, 2001.

[32] R. J. Aumann and J. H. Dreze, "Cooperative games with coalition structures," *Int. J. Game Theory*, vol. 3, no. 4, pp. 217–237, 1974. [Online]. Available: https://doi.org/10.1007/BF01766876

[33] R. M. Thrall and W. F. Lucas, "N-person games in partition function form," *Naval Res. Logist. Quart.*, vol. 10, no. 1, pp. 281–298, 1963. [Online]. Available: https://onlinelibrary.wiley.com/doi/abs/10.1002/nav.3800100126

[34] K. R. Apt and A. Witzel, "A generic approach to coalition formation," *Int. Game Theory Rev.*, vol. 11, no. 3, pp. 347–367, 2009.

[35] Y. Zhang *et al.*, "Context awareness group buying in D2D networks: A coalition formation game-theoretic approach," *IEEE Trans. Veh. Technol.*, vol. 67, no. 12, pp. 12259–12272, Dec. 2018.

[36] L. Ruan, J. Chen, Q. Guo, X. Zhang, Y. Zhang, and D. Liu, "Group buying-based data transmission in flying ad-hoc networks: A coalition game approach," *Information*, vol. 9, no. 10, p. 253, 2018.

[37] J. Dreze and J. Greenberg, *Hedonic Coalitions: Optimality and Stability*, Université Catholique Louvain, Center Oper. Res. Econometr., Ottignies-Louvain-la-Neuve, Belgium, Rep. 403, Jan. 1980. [Online]. Available: https://ideas.repec.org/p/cor/louvrp/403.html
[38] Y. Xu, J. Wang, Q. Wu, A. Anpalagan, and Y.-D. Yao, "Opportunistic spectrum access in cognitive radio networks: Global optimization using local interaction games," *IEEE J. Sel. Topics Signal Process.*, vol. 6, no. 2, pp. 180–194, Apr. 2012.
[39] D. Monderer and L. S. Shapley, "Potential games," *Games Econ. Behav.*, vol. 14, pp. 124–143, May 1996.
[40] Y. Xu, J. Wang, Q. Wu, J. Zheng, L. Shen, and A. Anpalagan, "Dynamic spectrum access in time-varying environment: Distributed learning beyond expectation optimization," *IEEE Trans. Commun.*, vol. 65, no. 12, pp. 5305–5318, Dec. 2017.
[41] P. Li and H. Duan, "A potential game approach to multiple UAV cooperative search and surveillance," *Aerosp. Sci. Technol.*, vol. 68, pp. 403–415, Sep. 2017.
[42] G. Arslan, J. R. Marden, and J. S. Shamma, "Autonomous vehicle-target assignment: A game-theoretical formulation," *J. Dyn. Syst. Meas. Control*, vol. 129, no. 5, pp. 584–596, 2007.
[43] G. Wang, G. Li, S. Tian, W. Dai, and J. Lv, "Multiple access strategy in cooperative localization network: Characteristics and examples," in *Lecture Notes in Electrical Engineering,* vol. 652. Chengdu, China: Springer, 2020, pp. 463–474. [Online]. Available: http://dx.doi.org/10.1007/978-981-15-3715-8_42.
[44] I. Pilaszy, D. Zibriczky, and D. Tikk, "Fast als-based matrix factorization for explicit and implicit feedback datasets," in *Proc. RecSys*, 2010, pp. 71–78. [Online]. Available: http://dx.doi.org/10.1145/1864708.1864726
[45] Q. Wu, Y. Xu, J. Wang, L. Shen, J. Zheng, and A. Anpalagan, "Distributed channel selection in time-varying radio environment: Interference mitigation game with uncoupled stochastic learning," *IEEE Trans. Veh. Technol.*, vol. 62, no. 9, pp. 4524–4538, Nov. 2013.

Lang Ruan received the B.S. degree in information and computing science from Zhejiang University, Hangzhou, China, in 2016, and the M.S. degree from the College of Communications Engineering, Army Engineering University of PLA, Nanjing, China, in 2019, where he is currently pursuing the Ph.D. degree.

His current research interests include game theory, UAV communications networks, and cooperative localization.

Guangxia Li received the B.S. and M.S. degrees from the Institute of Communication Engineering, Nanjing, China, in 1983 and 1986, respectively.

He is currently a Professor with the College of Communication Engineering, Army Engineering University of PLA, Nanjing. His current research interests include the design of communication systems, satellite communications, satellite navigation, communication anti-jamming, and satellite TT&C.

Weiheng Dai received the Ph.D. degree from the Institute of Communication Engineering, Nanjing, China, in 2004.

He is currently an Associate Professor with the College of Communication Engineering, Army Engineering University of PLA, Nanjing. His current research interests include the satellite navigation system and terminal technology, communication and navigation fusion technology, and cooperative positioning technology.

Shiwei Tian received the B.S. degree in electronic information engineering from Xidian University, Xi'an, China, in 2008, and the M.S. and Ph.D. degrees in communication and information system from the Army Engineering University of PLA, Nanjing, China, in 2011 and 2015, respectively.

Since 2015, he has been an Assistant Professor with the College of Communications Engineering, Army Engineering University and since 2021, he has been working with the National Innovation Institute of Defense Technology, Beijing, China. His main research interests are satellite navigation, satellite communication, and cooperative positioning.

Guangteng Fan received the Ph.D. degree from the College of Electronic Science and Engineering, National University of Defense Technology, Changsha, China, in 2016.

He has been working with the National Innovation Institute of Defense Technology, Beijing, China, since 2017, where he is a Lecturer of GNSS Signal Acquisition and Tracking.

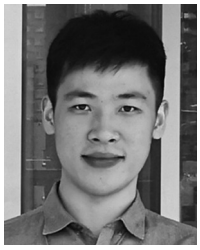

Jian Wang (Member, IEEE) received the Ph.D. degree in information and communication engineering from the National University of Defense Technology, Changsha, China, in 2017.

From September 2015 to September 2016, he was a Visiting Scholar with the Integrated Systems Laboratory, Swiss Federal Institute of Technology (ETH), Zürich, Switzerland. Since 2018, he has been a Research Associate with the National Innovation Institute of Defense Technology, Academy of Military Science, Beijing, China. His research interests are in the area of digital signal processing and special-purpose VLSI processor architectures.

Xiaoqi Dai received the bachelor's degree in applied physics from Xuzhou Institute of Engineering, Xuzhou, China, in 2014.

He is an Engineer, mainly engaged in hardware design and development. Since 2019, he has been working with the College of Communications Engineering, Army Engineering University of PLA, Nanjing, China, engaged in the application of satellite navigation and collaborative positioning